THERMOCHEMICAL TREATMENT OF PLATINUM GROUP METAL TAILINGS WITH AMMONIUM SALTS FOR MAJOR ELEMENT RECOVERY

Sameera Mohamed[1,2], Keabetswe Lehong[1], Elizabet M. van der Merwe[3], Wladyslaw Altermann[2,†], Frédéric J. Doucet[1]*

[1] Council for Geoscience, Private Bag X112, Pretoria 0001, South Africa

[2] Department of Geology, University of Pretoria, Lynnwood Road, Pretoria 0002, South Africa

([†] Kumba-Exxaro chair)

[3] Department of Chemistry, University of Pretoria, Lynnwood Road, Pretoria 0002, South Africa

*Corresponding author. Tel: +27 (0) 12 841 1300. E-mail address: fdoucet@geoscience.org.za

ORCID:

Sameera Mohamed:	0000-0003-0757-8254
Keabetswe Lehong:	0000-0003-3798-1749
Elizabet M. van der Merwe:	0000-0002-4452-1292
Wladyslaw Altermann:	0000-0002-9499-424X
Frédéric J. Doucet:	0000-0002-7980-476X

Abstract

It was recently demonstrated that the extraction of major elements from South African Platinum Group Metals (PGM) tailings can be achieved via thermochemical treatment with ammonium sulphate followed by aqueous dissolution. The current study uses the insight gained from the previous work and investigates and compares major element extraction efficiencies obtained using ammonium sulphate and three other ammonium salts (ammonium bisulphate *vs* ammonium chloride *vs* ammonium nitrate) as extracting agents at five different temperatures (350 to 550 °C). Overall, ammonium sulphate was the most promising reagent for the co-extraction of major elements, with the best extraction efficiencies achieved for aluminium (*ca.* 60%) and calcium (*ca.* 80%), alongside chromium (*ca.* 29%), iron (*ca.* 35%), magnesium (*ca.* 25%) and silicon (*ca.* 32%). In contrast, ammonium chloride and ammonium nitrate extracted smaller quantities of these elements, in particular chromium which was hardly extracted (≤ 1.2%), whereas calcium was nearly equally extracted for all salts (70-80%). It could not be ascertained whether the plagioclase phase, as anorthite, reacted with ammonium salts during the thermochemical step, but it was found to dissolve nearly completely during the acid leaching step in the absence of thermochemical processing. This phase was the main contributor to calcium and aluminium in solution. The greatest effect of temperature was on the flowability characteristic of the reaction product after treatment rather than on elemental extraction efficiencies. Thermochemical treatment using ammonium sulphate represents the most promising route for extracting valuable elements from PGM tailings, which could be subsequently converted to value-added products.

Keywords

PGM tailings; ammonium salts; elemental extraction; thermochemical treatment; solid-solid treatment

1. Introduction

The storage and handling of vast volumes of solid waste generated by the mining sector is increasingly linked to major environmental and economic issues. In the context of reducing the environmental burden and enhancing economic benefit, which are part of the expected contributions of mining to the emerging circular economy [1,2], the development of new technologies for converting mineral and mining waste to value-added products is rapidly becoming an important priority research area at government institutions (*e.g.* Europe [3]; South Africa [4]). This is also evidenced by the growing number of recent publications which address the potential use

of mine waste as secondary resources of valuable minerals and metals (e.g. PGM tailings [5–7]; bauxite [8,9]; copper tailings [10]; iron ore tailings [11]; anorthosite tailings [12]).

In South Africa, the scale of tailings production associated with the primary production of Platinum Group Metals (PGMs) in the Bushveld Igneous Complex (BIC) is extensive and approaches 80 Mt p.a. [13]. These alkaline tailings are regarded as hazardous waste. While the regulations pertaining to mine waste has evolved considerably over the last five years, mine tailings have also been increasingly reprocessed for the recovery of additional primary commodities, mostly precious and ferrous metals (e.g. gold, PGM's). A typical example is the largest PGM beneficiation plant of surface chrome tailings, which produces platinum, palladium, rhodium and gold concentrates using the ConRoast process [14]. Two other examples are the beneficiation plant at the Two Rivers Platinum mine, which has been recovering chromite from its PGM tailings since 2013 [15], and the new R100-million tailings retreatment project for the recovery of chromium from Northam's Booysendal South tailings storage facility [16]. Mg-rich tailings from the South African Bushveld Igneous Complex (BIC) have been identified as potential resources for CO_2 mineralisation [5,13,17]. These same tailings also contain > 10% Al and may therefore represent suitable alternatives to Al import or to coal fly ash as secondary Al resource [18,19], since South Africa is deprived of economically-mineable bauxite deposits for the supply of the metal [20]. The content of iron in PGM tailings (> 20%) means that these residues may also represent secondary sources of the metal [6].

There are currently no known commercial processes for the extraction of major elements from South African PGM tailings. Such elements are Al, Ca, Cr, Fe and Mg. In line with their effort to sustainability of the country's mineral resources, the Council for Geoscience, in partnership with the University of Pretoria, has developed a promising, two-stage process for the extraction of major elements from PGM tailings [6,7]. The first stage involves solid-solid thermochemical treatment of PGM tailings in the presence of ammonium sulphate ($(NH_4)_2SO_4$), a widely available, low-cost, recyclable chemical agent. The chemical affinity between $(NH_4)_2SO_4$ and major elements present in the tailings leads to the formation of water-soluble sulphate-metal species. The second stage of the process uses dilute acid below 100 °C to dissolve the sulphate-metal species. At this stage of development, the method suffers from a lack of elemental selectivity, with several metals competing for SO_4^{2-} ions during the thermochemical step. This may however be of advantage in recovering several valuable metals for further processing, as an important step towards achieving the full potential of utilisation of PGM tailings.

In recent years, the extractive properties of other ammonium salts under thermal conditions have been tested on several mineral-bearing materials. For instance, ammonium bisulphate (NH_4HSO_4) was shown to be better suited than $(NH_4)_2SO_4$ for the extraction of Mg from serpentine and metaperidotite minerals [21], and under some conditions for the extraction of Al from coal fly ash [19]. Valuable metals were also successfully extracted from copper ores [22], nickel ores [23], and copper smelter slag [24] via thermochemical treatment with ammonium chloride (NH_4Cl). It was therefore of interest to assess whether other ammonium salts may be more suitable than $(NH_4)_2SO_4$ for major element extraction from PGM tailings, even though the mineralogy of PGM tailings differs greatly from that of other materials studied.

This paper is a follow-up to previous studies [6,7]. The primary objective of this paper was to test and compare the suitability of several ammonium salts for major element extraction from PGM tailings via thermochemical treatment. An outline of the multi-stage extraction process is illustrated in Figure 1. In continuity with the previous work, the same PGM mine tailings sample from the two Rivers mine was used as a case study.

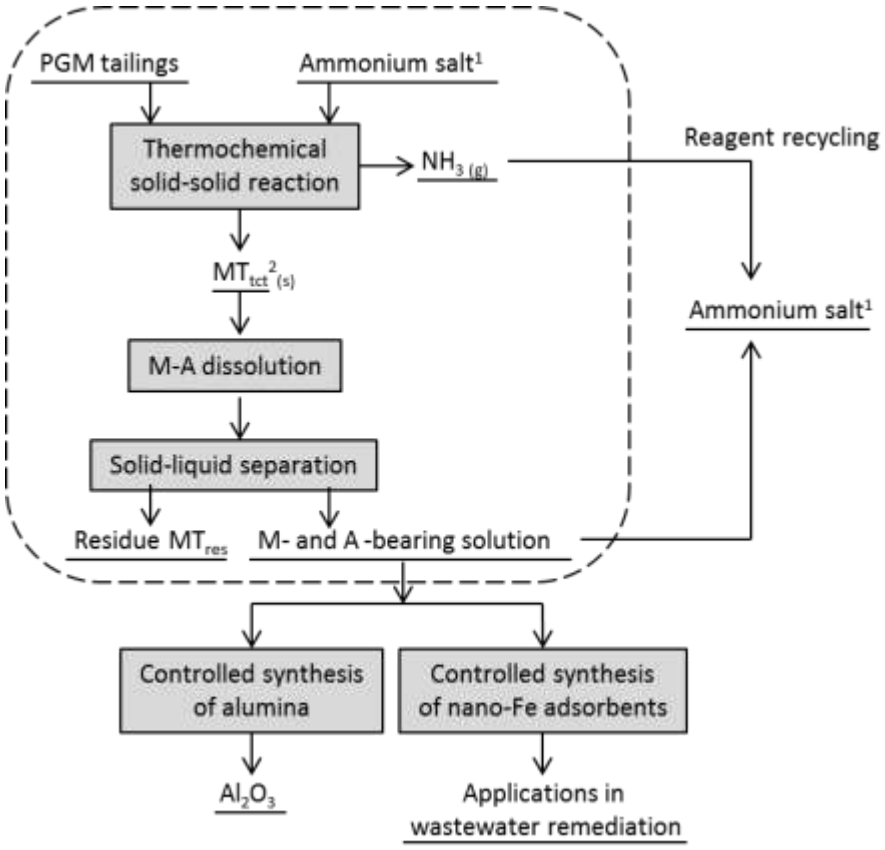

Figure 1. Process flow diagram for the multi-stage extraction of major elements from PGM mine tailings ([1] Ammonium salts tested: $(NH_4)_2SO_4$, NH_4HSO_4, NH_4Cl, NH_4NO_3; [2] MT_{tct} contains M-A compounds, where M is a metal and A is the anion from the salt used (*i.e.* SO_4^{2-}, Cl^- or NO_3^-); the highlighted area represents the focus of this study).

2. Experimental section

2.1. Material tested

Preparation and detailed characterisation (using XRD, XRF, TG and FE-SEM) of the tailings sample used in this study were performed and were described elsewhere [6]. In short, the sample originated from the Two Rivers Platinum Mine located in the southern sector of the eastern limb of the Bushveld Igneous Complex (BIC; Mpumalanga, South Africa). Following up on our previous study, all experiments were performed using the 45-75 µm size fraction (hereafter called $MT_{45\text{-}75}$) of the sample. The mineralogical composition of $MT_{45\text{-}75}$ was dominated by spinel group minerals (29.5%; most probably magnetite, chromite and ulvöspinel [25]), orthopyroxene (27.8%; as enstatite) and plagioclase (25.2%; as anorthite). $MT_{45\text{-}75}$ also contained amphibole (7.9%; as hornblende), and several alteration minerals, namely chlorite (3.1%), talc (1.0%) and serpentine (trace), albeit in much smaller proportions. Minor primary minerals included clinopyroxene (1.7%; as augite) and mica (1.6%). The most abundant elements identified in $MT_{45\text{-}75}$ included Cr_2O_3 (31.9%), $Fe_2O_{3\ (tot)}$ (23.3%), MgO (13.6%), Al_2O_3 (12.2%) and SiO_2 (17.4%). The sample contained 2.5% CaO. Low modal abundances (≤ 0.7%) were reported for MnO, Na_2O, K_2O and TiO_2. The sample exhibited a slightly negative loss on ignition (LOI = -1.3%), which was ascribed to the oxidation of ferrous iron (Fe^{2+}) contained in e.g. spinel group minerals, to ferric ion (Fe^{3+}) [6].

2.2. Thermochemical treatment (static furnace)

$MT_{45\text{-}75}$ was mixed thoroughly with different ammonium salts, i.e. ammonium sulphate ($(NH_4)_2SO_4$; reagent grade, ≥ 99%, Merck, South Africa); ammonium bisulphate (NH_4HSO_4, reagent grade, ≥ 98% , Sigma Aldrich, United Kingdom); ammonium chloride (NH_4Cl; reagent grade, ≥ 99.8%, Merck, South Africa); and ammonium nitrate (NH_4NO_3; reagent grade, ≥ 99%, Sigma Aldrich, United Kingdom), at a constant solid-solid mass ratio of 2:6 (m/m), using an established preparation method [6]. The resulting mixtures were placed in fused quartz crucibles and were subsequently heat-treated in a muffle furnace set at varying temperatures (350, 400, 450, 500 or 550 °C) for 45 minutes. The products of the reaction (hereafter denoted MT_{tct}) were allowed to cool down to 25 °C and were ground using a mortar and pestle before characterization and subsequent treatment.

2.3. Dissolution procedures

All MT_{tct} samples were subjected to a dissolution procedure described elsewhere [6]. Briefly, the procedure consisted of suspending 3.00 ± 0.02 g (dry mass) of MT_{tct} in 0.63 M HNO_3 solution at 95 °C

under continuous mixing conditions for 6 hours. Dissolution of MT_{tct} generated at 550 °C using all salts was also performed in ultrapure water (electrical conductivity < 1 µS cm^{-1}) either at 25 °C and 95 °C for 1 and 6 hours, for comparative purpose. At the end of the dissolution period, the leachates were filtered under reduced pressure. The filtrates were subsequently analysed for their major elements content by inductively coupled plasma optical emission spectrometry (ICP-OES) at an accredited laboratory (Waterlab Pty Ltd, Pretoria, South Africa).

2.4. Characterization of solid materials

TG and DTA analyses were performed on a TA Instruments Q600 SDT. A multipoint temperature calibration was performed using indium, zinc and gold calibration standards. Mass calibration was carried out using the manufacturer supplied calibration mass set. Approximately 20 mg of sample was heated from 25 to 1000^{o}C at a heating rate of 10^{o}C min^{-1} in alumina pans under a dynamic air atmosphere, controlled at a flow rate of 100 ml min^{-1}. Analyses were performed in duplicate to confirm the observed effects.

Chemical and mineralogical compositions of untreated tailings (MT_{45-75}) and leach residues (MT_{res}) were obtained using XRF (PANanalytical AxiosX-ray fluorescence spectrometer equipped with a 4 kW Rh tube) and XRD (Bruker D8 Advance X-ray diffractometer), respectively. The samples were micronized to a particle size < 30 µm for increased accuracy prior to XRD analysis. Phase concentrations were determined by Rietveld quantitative analysis with DIFFRAC TOPAS software.

Field-emission scanning electron micrographs (FE-SEM) were collected using a Gemini® Ultra Plus Field Emission microscope (Carl Zeiss, Germany) operating under high-vacuum condition with an accelerating voltage of 1.0 kV to obtain information on morphologies and size distribution of all solid materials. Samples were mounted on a metal substrate by means of a double-sided carbon tape and subsequently sputter-coated with a thin, conductive layer of carbon using an Emitech K550X coater (Ashford, England).

3. Results and Discussion

3.1. Thermogravimetric analysis of ammonium salts

In order to better understand the process of thermochemical treatment of PGM tailings with ammonium salts, it is important to gain insight on the thermal decomposition of the pure ammonium salts used over the temperature range studied, since it will affect the thermochemical

process. However, the nature, kinetics and combination of decomposition reactions taking place for the different salts when subjected to thermal treatment, and the extent of their occurrences are complex. They strongly depend on experimental conditions *(e.g.* sample size, heating rate) which regulate them, and as a result cannot be described by any single and/or simple mechanistic process. Although a detailed study of the mechanisms of thermal decomposition of the four ammonium salts is outside the scope of this paper, differences in their thermal behaviours were illustrated using TG in combination with DTA (Figure 2), and the results were compared to the published literature. Possible decomposition mechanisms for the different salts are summarised in Table 1 and discussed below.

The decomposition mechanism of $(NH_4)_2SO_4$ has been discussed at length in our previous work [6]. The decomposition undergoes three distinct stages (Table 1, Eqns. 1-15): (1) a process of deammoniation corresponding to the loss of ammonia (NH_3) and to the formation of ammonium bisulphate (NH_4HSO_4) and/or triammonium bisulphate ($(NH_4)_3H(SO_4)_2$); (2) the decomposition of NH_4HSO_4 into ammonium pyrosulphate ($(NH_4)_2S_2O_7$) or the formation of sulphamic acid (NH_2SO_3H) as an intermediate prior to the formation of $(NH_4)_2S_2O_7$); and (3) the decomposition of $(NH_4)_2S_2O_7$ into gaseous products (NH_3, SO_2, H_2O, N_2) ([6]; and references therein). The TG and DTA curves obtained for the decomposition of $(NH_4)_2SO_4$ (Figure 2) showed a number of mass loss events and endothermic peaks in the temperature range 200-650 °C, which were indicative of a multi-step decomposition mechanism. Only two mass loss transitions could be identified in the region 200 – 500 °C from the TG result, but the DTA curve indicated the occurrence of at least four different transitions in the same temperature range. Characterisation of these transitions and those observed for all other ammonium salts described later may be studied with the aid of complementary techniques (TG-FTIR, TG-MS or TG-GC), but falls outside the scope of this paper.

NH_4HSO_4 is a decomposition product of $(NH_4)_2SO_4$ and its decomposition mechanism follows from the above-mentioned steps (2) and (3) of $(NH_4)_2SO_4$ decomposition (Table 1, eqns. 16-21). An alternative decomposition process was also proposed [26], which would involve the dissociation of NH_4HSO_4 into NH_3 and H_2SO_4 (Table 1, eqn. 22); the latter decomposition product would then fuse with various oxides to form metal-sulphate based compounds. The TG results obtained for the decomposition of NH_4HSO_4 (Figure 2A) indicated that the mass of NH_4HSO_4 has remained stable up to 210 °C before decreasing by 95% at 440 °C. The DTA curve (Figure 2B) indicated the presence of two endothermic peaks at 153 °C and 440 °C respectively. The first peak was not associated with any mass loss in the TG curve (Figure 2A) and could be ascribed to melting of NH_4HSO_4 [27]. Its decomposition (with a corresponding loss of mass in the TG curve) into ammonium pyrosulphate

($(NH_4)_2S_2O_7$), or its recrystallization and subsequent formation of non-equilibrium phases such as NH_2SO_3H or $(NH_4)_2S_2O_7$, followed by decomposition of $(NH_4)_2S_2O_7$ into gaseous decomposition products (NH_3, SO_2, H_2O, N_2), would then follow and reach the maximum rate at 440 °C.

In comparison to the other ammonium salts, the mechanism of thermal decomposition for NH_4Cl described in the published literature is a fairly simple reversible process (Eqn 23; Table 1). The salt is thermally stable up to about 185 °C, at which temperature it undergoes a change in crystal structure, which is in principle indicated by an endothermic event in the DTA curve. This is followed by sublimation starting from 200 °C, which results in the formation and loss of gaseous decomposition products, NH_3 and HCl respectively. The HCl released during decomposition is very reactive with various metal oxides at temperatures above 300°C to form metal-based chloride compounds [26,28,29]. The TG curve (Figure 2A) obtained in this study indicated an onset of decomposition of NH_4Cl slightly below 200°C, with a 95% mass loss reached at 330 °C. The DTA curve (Figure 2B) indicated the presence of two endothermic events with maxima at 202 °C and 310 °C respectively, which indicated the change in crystal structure and sublimation of NH_4Cl described earlier.

The decomposition mechanism of NH_4NO_3 is particularly complex, with experimental conditions e.g. sample size, heating rate, purity, determining the decomposition characteristics and products formed [30]. For this reason, only a brief overview of the thermal stability and main decomposition reactions will be provided here. In its solid form, NH_4NO_3 undergoes two structural transformations above room temperature, i.e. T≈ 58 °C and 132 °C, before melting at 169 °C [31]. The literature generally agrees that thermal decomposition is initiated by an endothermic proton transfer reaction, forming NH_3 and HNO_3, as described by Eq. 24 (Table 1). Exothermic decomposition then occurs from 200-230 °C and has been described to occur via Eq. 25, although the reactions described in Eqns. 26-29 are also possible [30–32]. TG curves (Figure 2A) indicated that NH_4NO_3 had the lowest decomposition temperature of the four ammonium salts studied. The mass of NH_4NO_3 remained relatively constant up to 200 °C, before losing 95% of its mass between 200 °C and 310 °C. The DTA curve (Figure 2B) indicated the presence of four endothermic peaks, which were indicative of two structural transformations with peak maxima at 55 and 133 °C, melting at 165 °C, and decomposition of molten NH_4NO_3 with a peak maximum at 326 °C, confirming the results obtained earlier [31].

Table 1. Equations describing possible decomposition reactions sustained by ammonium salts when subjected to thermal treatment.

Possible Decomposition Reactions	
Ammonium sulphate ($(NH_4)_2SO_4$) [26,46–49]	
Reaction system 1 [46–48]	
(NH4)2SO4(s) → NH4HSO4 (s) + NH3(g)	(1)
2(NH4)2SO4(s) → (NH4)3H(SO4)2(s) + NH3(g)	(2)
(NH4)2SO4(s) + NH4HSO4(s) → (NH4)3H(SO4)2(s)	(3)
(NH4)3H(SO4)2(s) → (NH4)2S2O7(s) + NH3(g) + H2O(g)	(4)
$2NH_4HSO_4(s) \rightarrow (NH_4)_2S_2O_7(s) + H_2O(g)$	(5)
3(NH4)2S2O7(s) → 2NH3(g) + 6SO2(g) + 9H2O(g) + 2N2(g)	(6)
Overall equation: 3(NH4)2SO4(s) → 4NH3(g) + 3SO2(g) + 6H2O(g) + N2(g)	(7)
Reaction system 2 [46,49]	
(NH4)2SO4 (s) → NH4HSO4 (s) + NH3 (g)	(8)
2(NH4)2SO4 (s) → (NH4)3H(SO4)2 (s) + NH3 (g)	(9)
NH4HSO4 (s) ↔ NH2SO3H (s) + H2O (g)	(10)
NH2SO3H(s) + NH4HSO4(s) → (NH4)2S2O7(s)	(11)
$2NH_4HSO_4(s) \rightarrow (NH_4)_2S_2O_7(s) + H_2O(g)$	(12)
3(NH4)2S2O7(s) → 2 NH3(g) + 6SO2(g) + 9H2O(g) + 2N2(g)	(13)
Reaction system 3 [26]	
(NH4)2SO4(s) → NH4HSO4 (s) + NH3(g)	(14)
$NH_4HSO_4(s) \rightarrow H_2SO_4(g) + NH_3(g)$	(15)
Ammonium bisulphate (NH_4HSO_4) [26,46–49]	
Reaction system 1 [46–48]	
$2NH_4HSO_4(s) \rightarrow (NH_4)_2S_2O_7(s) + H_2O(g)$	(16)
3(NH4)2S2O7(s) → 2NH3(g) + 6SO2(g) + 9H2O(g) + 2N2(g)	(17)

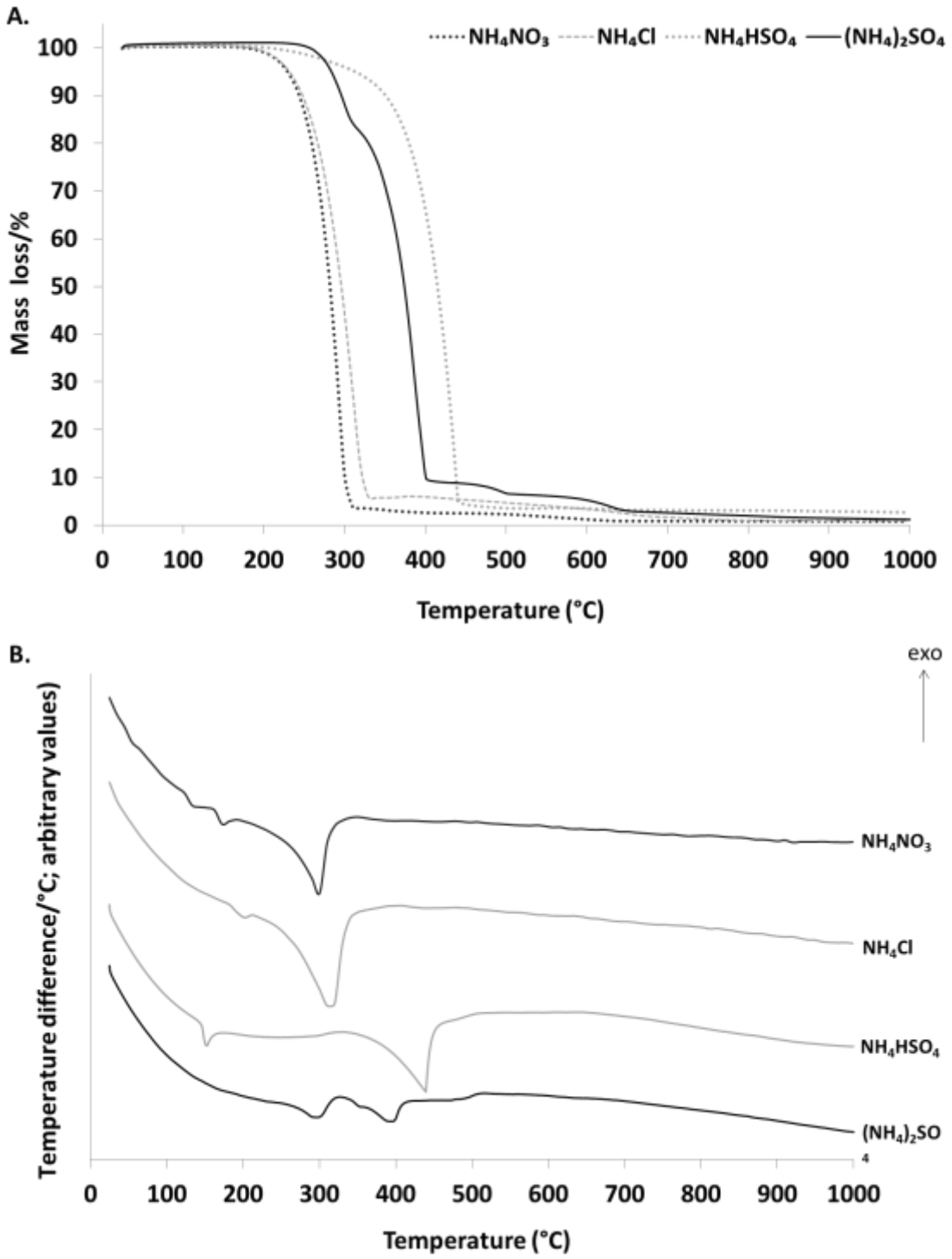

Figure 2. TG (A) and DTA (B) curves for different ammonium salts (NH_4Cl; NH_4NO_3; NH_4HSO_4; and $(NH_4)_2SO_4$) under dynamic temperature conditions (heating rate of 10 °C/min in air).

3.2. Dissolution experiments

As conveyed previously [6], major elements such as Al_2O_3, CaO, Fe_2O_3, MgO and Cr_2O_3 can be extracted from PGM tailings via thermochemical treatment followed by aqueous dissolution. The

thermochemical treatment step used in the previous study made use of $(NH_4)_2SO_4$ as extracting agent at 550 °C. In the present follow-up study, the suitability of other ammonium salts for major element extraction was tested and compared to that of $(NH_4)_2SO_4$ at varying temperatures. Direct quantitative comparison between extraction efficiencies achieved by the different salts and different temperatures was performed by adopting the same dissolution technique as used previously. In the earlier study, dissolution of thermochemically treated PGM tailings (MT_{tct}) in ultra-pure water promoted the formation of secondary Fe precipitates, which in turn prevented the quantification of the efficiency of the thermochemical treatment for elemental extraction, in particular for Fe. The secondary precipitation was prevented by leaching MT_{tct} in 0.63M HNO_3 solution at 95 °C for 6h [6]. This improved dissolution procedure was therefore adopted.

As a baseline, leaching of untreated MT_{45-75} using this procedure was also performed as a control [7] in order to ascertain the respective contribution of the thermochemical step *vs* the acid dissolution step to elemental extraction. The dissolution step, when applied to MT_{45-75} in the absence of the preceding thermochemical step, was found to extract (i) little Cr (0.1 %) and Fe (2.9 %); (ii) some Mg (9.1 %), Al (27.0 %) and Si (29.9%); and (iii) a substantial amount of Ca (69.0 %) contained in the tailings sample [7]. As a follow-up, the present study also complemented these extraction data for the control experiment, by reporting XRD analysis of the corresponding MT_{res} sample (Section 3.3.1). This provided insight on the most reactive mineral phases present in MT_{45-75} during the acid dissolution step.

3.2.1. Dissolution in HNO_3 solution

Extracting agent: $(NH_4)_2SO_4$

When compared to the above control experiment, it was found that coupling the thermochemical step using $(NH_4)_2SO_4$ at 550 °C for 45 min with mild acid dissolution enhanced the extraction of Cr to 26.9 %, Fe to 34.7 %, Mg to 25.2 %, Al to 59.1 %, and Ca to 80.0% [6]. However, this thermochemical step performed at 550 °C failed to improve Si extraction (30.5 %). These findings revealed that (i) most of the silicon and calcium are extracted via the acid leaching step, (ii) aluminium and magnesium are extracted at each stage of the process, and (iii) the thermochemical step is the main contributor to chromium and iron extraction [7]. The Si results also prompted to suggest a lack of reactivity between Si-O bonds contained in the tailings and $(NH_4)_2SO_4$ at this temperature [7], albeit this may not be the case at lower treatment temperatures. The extent of this chemical affinity, or

lack thereof, between Si-O bonds present in the PGM tailings and $(NH_4)_2SO_4$ as a function of temperature was therefore also tested.

As a result, elemental co-extraction demonstrated that several metals had a strong chemical affinity for the sulphate molecule of $(NH_4)_2SO_4$ during the thermochemical treatment step. Similar observations were made for serpentinite rocks [21,33,34]. It also indicated that the metals competed for the extracting agent to form water-soluble NH_4^+-M-SO_4^{2-} and M^{2+}-SO_4^{2-} species. However, the thermodynamics involved in the competitive extraction mechanisms were most likely influenced by the temperature used during thermochemical treatment (T_{tct}). In the previous study, a qualitative assessment of the effect of T_{tct} was performed, with the aim of selecting a favourable T_{tct} for the optimisation of the subsequent dissolution procedure. A T_{tct} of 550 °C was selected since it appeared to promote reaction completeness between $MT_{45\text{-}75}$ and $(NH_4)_2SO_4$ for the duration of the experiment, on the basis of several qualitative observations made at T_{tct} between 350 °C and 550 °C (*i.e.* flowability characteristic of solid MT_{tct}; mass losses recorded at the end of thermochemical treatment; TG and qualitative XRD analyses of MT_{tct}) [6].

Ultimately, elemental extraction efficiencies obtained from ICP analyses of leachates are more accurate to confirm the efficiency of the thermochemical treatment. For this reason, MT_{tct} produced at different T_{tct} varying between 350 °C and 550 °C were subjected to the dissolution procedure and element extraction efficiencies for Al, Ca, Cr, Fe, Mg and Si were determined (Figure 3). The extent of extraction for Al, Fe and Mg was the highest at the T_{tct} of 550 °C (59.1%, 34.7% and 25.2% respectively). A noteworthy observation was that Si extraction was enhanced at temperatures ≤ 400 °C (38.7% at 350 °C), when compared to the extent of extraction observed at higher temperatures, or in the absence of the thermochemical step (*i.e.* control using acid leaching only). This indicated some degree of reactivity between some silicate and/or aluminosilicate frameworks contained in these materials and $(NH_4)_2SO_4$ at temperatures ≤ 400 °C, but not in the range 450-550 °C. This is in contrast to the absence of reactivity we previously established between Si-O bonds in the amorphous alumina silica glassy matrix of South African fly ash and $(NH_4)_2SO_4$, where little Si (≤0.6%) had been extracted for T_{tct} values ranging between 400 °C and 600 °C [18], although the dissolution step in this work was performed in water at ambient temperature rather than in 0.63M HNO_3 solution at 95 °C. Romão et al. [34] also reported little (0.8%) Si extracted from Portuguese serpentinite. Regardless of T_{tct}, the best extraction efficiencies were achieved for Al (54.0-59.1%) and Ca (75.7-82.2%). However, the broad range of tested T_{tct} (i.e. 350 to 550 °C) was found to affect extraction efficiencies only within a limited margin (≤ 5.1% for Al, Cr and Fe; 8.5% for Ca and 9.0% for Si) when the duration of thermochemical treatment was 45 min. In addition to the economic

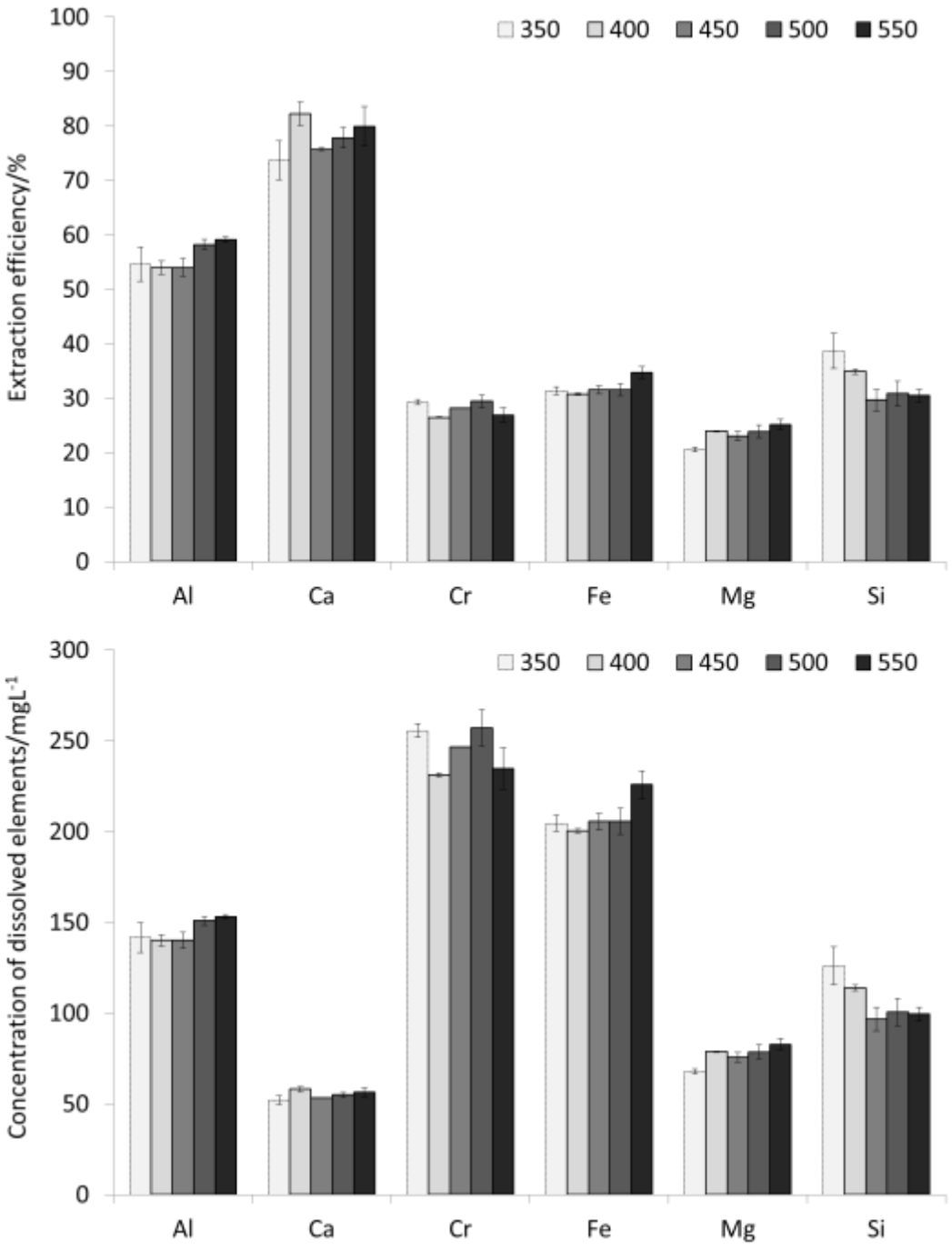

Figure 3. Effect of temperature used during thermochemical treatment of $MT_{45\text{-}75}$ with $(NH_4)_2SO_4$ ($MT_{45\text{-}75}$:$(NH_4)_2SO_4$ of 2:6; 45 min) on elemental extraction efficiency (A) and dissolved element concentration (B) following dissolution under controlled acid (0.63M HNO_3) condition (3 g MT_{tct}/500ml; 95 °C; 850 rpm; *n* = 2). The legend displays the thermochemical treatment temperatures (Source for data obtained at 550 °C: [6]).

considerations that must be taken into account, the physical properties of MT_{tct} represent an important factor to consider when selecting the most favourable T_{tct} for future applications of this process. Mohamed et al. [6] reported that at elevated T_{tct} (≥450 °C) MT_{tct} were free-flowing powders that were easily recovered. In contrast, at lower temperatures, MT_{tct} displayed a molten, viscous-like appearance when hot, i.e. immediately upon removal from the furnace, and hardened to resemble solid glassy blocks which had "fused" to the walls of the crucible upon cooling; the latter made the recovery process of the reaction products challenging. These observations were in agreement with other authors who investigated the thermochemical treatment of serpentinite rocks with $(NH_4)_2SO_4$ [21,35]. Increasing the duration of thermochemical treatment from 45 min to 6h at T_{tct} of 350 °C or 400 °C did not prevent the generation of hardened MT_{tct}, and lowered extraction efficiencies for most elements (Figure 4).

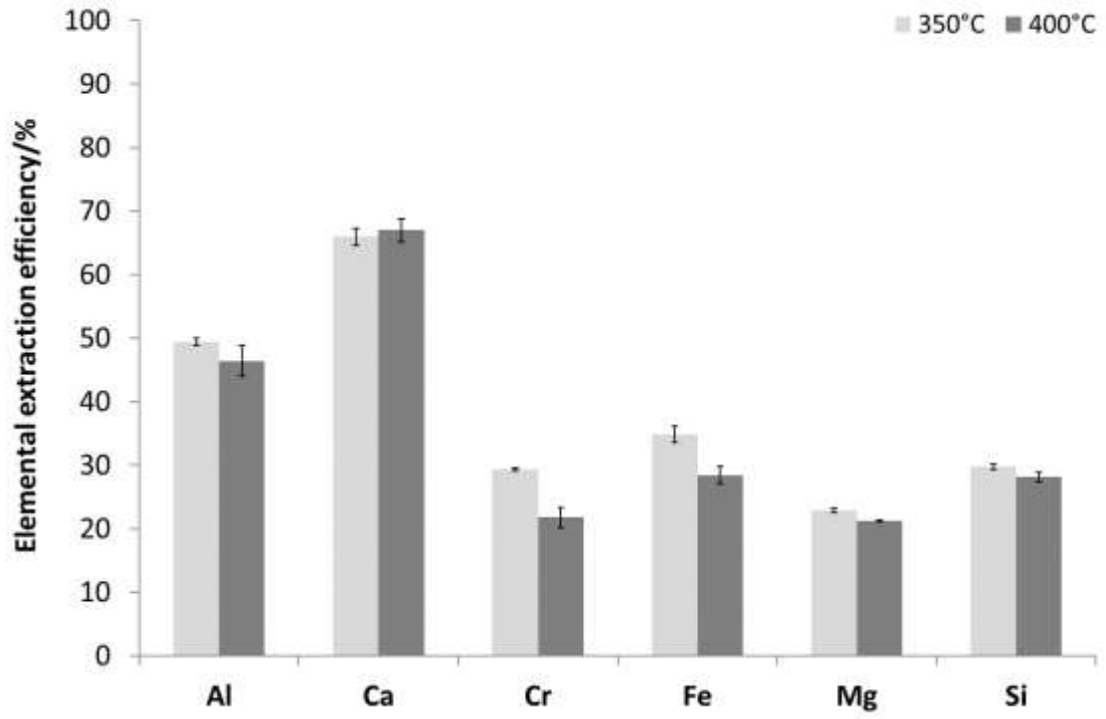

Figure 4. Elemental extraction efficiencies when using a reaction time of 6h for thermochemical treatment at 350 °C and 400 °C (MT_{45-75}:$(NH_4)_2SO_4$ of 2:6) followed by dissolution under controlled acid (0.63 M HNO_3) condition (3 g MT_{tct}/500ml; 95 °C; 850 rpm; *n* = 2).

Extracting agent: NH_4HSO_4

Another extracting agent, NH_4HSO_4, has recently been shown to promote faster and higher Mg extraction rates than $(NH_4)_2SO_4$ from Portuguese serpentinite and metaperidotite, especially for T_{tct} < 450 °C [21]. It was also found to improve the extraction of Al from coal fly ash under some processing conditions [19]. Although the mineralogy of these materials (serpentinite,

metaperidotite, and coal fly ash) is different to that of South African PGM tailings, it was important to test the effectiveness of NH_4HSO_4 as an alternative agent for the Two Rivers tailings sample. NH_4HSO_4 was found to be substantially less effective than $(NH_4)_2SO_4$ in extracting major metals (*i.e.* Al, Ca, Cr, Fe, Mg) at all temperatures tested (350 °C ≤ T_{tct} ≤ 550 °C) (Figure 5). The same trend was observed for Si when using a T_{tct} of 350 °C, but paradoxically, the extent of Si extraction was greater when using NH_4HSO_4 at T_{tct} ≥ 400 °C in lieu of $(NH_4)_2SO_4$, with as much as 44.3% being extracted at T_{tct} of 400 °C. This was a strong indication that the distinct mineralogical characteristics of the South African PGM tailings tested, which did not contain serpentine, metaperidotite or amorphous aluminosilicate phases, represented a key factor in the selection of the most appropriate extracting agent.

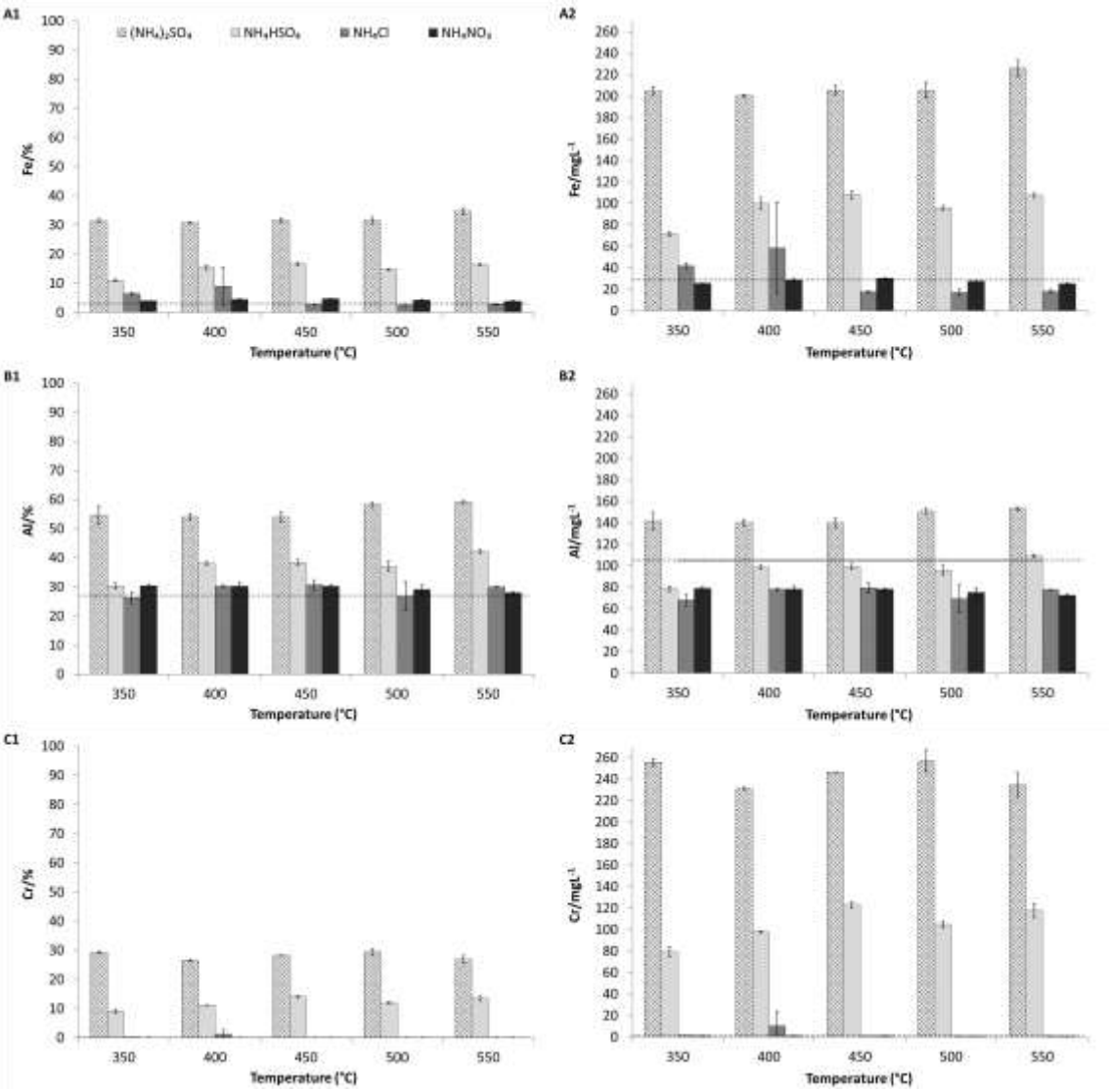

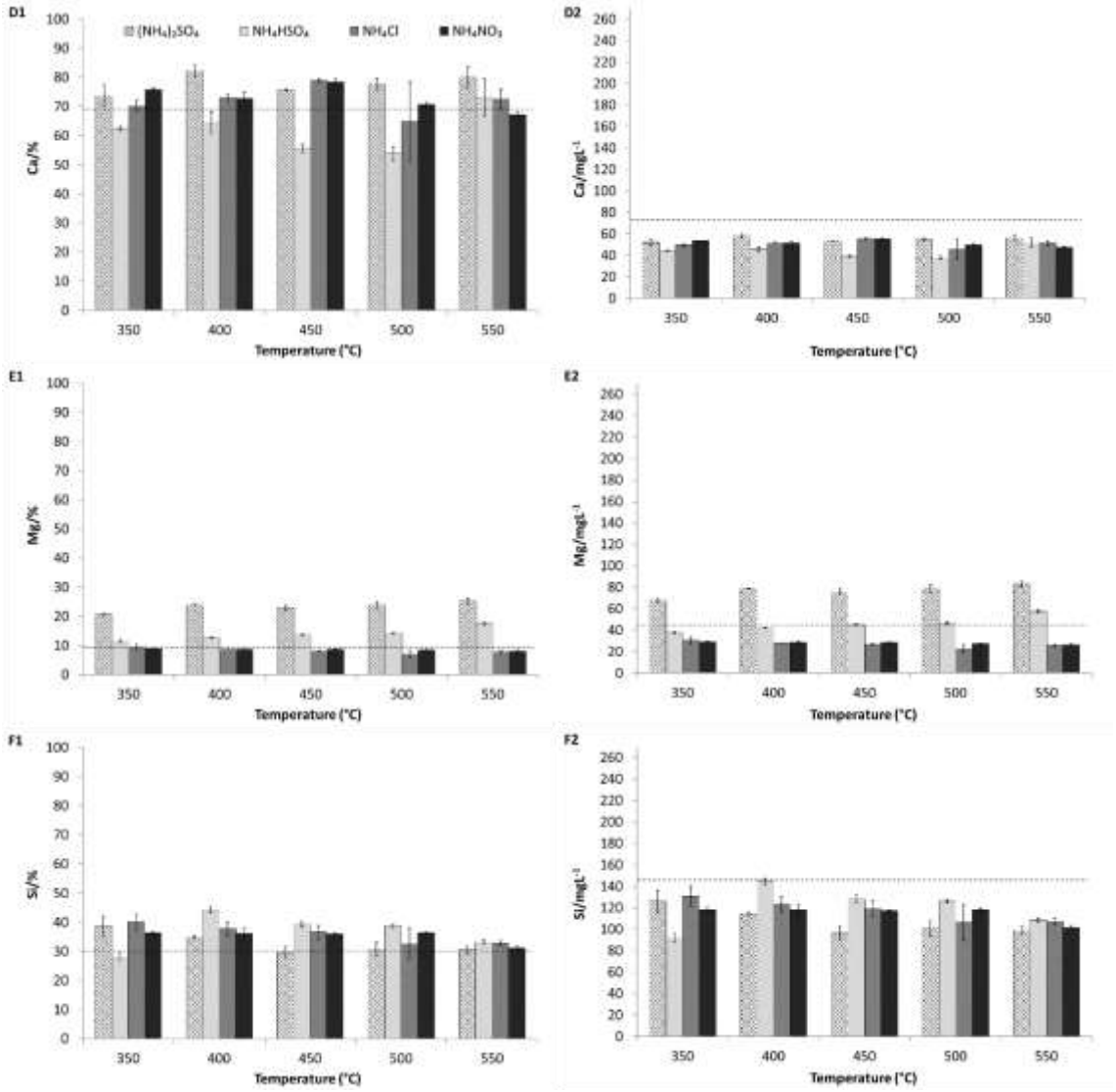

Figure 5. Effect of ammonium salt and temperature used during thermochemical treatment of $MT_{45\text{-}75}$ with ammonium salts ($MT_{45\text{-}75}$:salt of 2:6; 45 min) on elemental extraction efficiency (A) and dissolved element concentration (B) following dissolution under controlled acid (0.63 M HNO_3) condition (3 g MT_{tct}/500ml; 95 °C; 850 rpm; *n* = 2). Source for data obtained for $(NH_4)_2SO_4$ at 550 °C: [6]. The horizontal dashed lines represent elemental extraction for the control solution (*i.e.* acid dissolution only; data source: [7]).

Extracting agents: NH_4Cl and NH_4NO_3

NH_4Cl is another agent which has been shown to successfully extract valuable metals from materials such as copper ores [22], nickel ores [23] and copper smelter slag [24]. Given that NH_4HSO_4 did not yield better elemental extraction efficiencies than $(NH_4)_2SO_4$, the usefulness of NH_4Cl in recovering major elements from PGM tailings was also tested, and compared to that of NH_4NO_3, another ammonium salt which has not been previously investigated. Extraction efficiencies and concentrations of dissolved elements obtained with the two salts are reported in Figure 5. Both

NH_4Cl and NH_4NO_3 were unsuitable for Cr and Mg recovery from PGM tailings, with only 0.1% and ≤ 9.4% respectively extracted under all temperature conditions, which are identical to the values obtained in the absence of thermochemical treatment [7]. These results suggested that the two salts had little affinity for Cr-bearing spinels and for Mg-rich enstatite present in the tailings. Fe extraction was equally much lower when using NH_4Cl and NH_4NO_3, with values ≤ 9.0% in comparison to up to 34.7% recorded for $(NH_4)_2SO_4$. These values were nevertheless greater than those obtained for the control solution (2.9 %), which indicated some degree of reactivity between the two salts and Fe-bearing mineral phases present in the tailings sample. A similar trend was observed for Al, with extraction efficiencies approximating 30% with the two salts, compared to 27% for the control and 60% when using $(NH_4)_2SO_4$ as extracting agent. As observed for $(NH_4)_2SO_4$, Si extraction using NH_4Cl and NH_4NO_3 at 550 °C was identical to that observed for the control solution, and it increased by up to *ca.* 10% with decreasing temperature. Thermochemical treatment using the two salts at 550 °C did increase Ca concentration in solution, when compared to the data for the control solution, although it increased Ca extraction to ca. 80% at 450 °C.

Overall, ammonium sulphate was the most promising reagent for the co-extraction of major elements, with the best extraction efficiencies achieved for Al (*ca.* 60%) and Ca (*ca.* 80%), alongside Cr (*ca.* 29%), Fe (*ca.* 35%), Mg (*ca.* 25**%**) and Si (*ca.* 32%).

3.2.2. Dissolution in H_2O

The extraction data reported in Section 3.2.1 were obtained for a dissolution procedure using a 0.63M HNO_3 solution at 95 °C under continuous mixing conditions for 6 hours, which had been developed and optimised specifically for MT_{tct} samples that had been generated from the reaction between $MT_{45\text{-}75}$ and $(NH_4)_2SO_4$ salt [6]. However, this procedure may not have been optimal for MT_{tct} samples generated using the three other ammonium salts. For this reason, dissolution of the samples generated at 550 °C using all salts was also performed in ultrapure water at 25 °C and 95 °C, for 1 and 6 hours, for comparative purpose. Regardless of the temperature and duration of dissolution, higher extraction efficiencies were obtained for Fe, Al, Cr, Ca, Mg and Si when immersing MT_{tct} in HNO_3 rather than in H_2O (Supplementary Figure 1). These results confirmed that the dissolution procedure previously optimised for $(NH_4)_2SO_4$ salt [6] can also be successfully applied to MT_{tct} generated from the reaction between $MT_{45\text{-}75}$ and the three other salts.

3.3. Characterisation of thermochemically-treated tailings (MT_{tct}) and non-dissolved residues (MT_{res})

3.3.1. Control experiment

The control experiment revealed that elemental extraction efficiencies achieved using thermochemical treatment followed by the optimal dissolution procedure cannot be solely ascribed to the effect of the thermochemical step for all major elements ([7] and Figure 5). The mineral phases that contributed to elemental extraction in this control experiment were yet to be identified. In this follow-up study, XRD revealed little, if any, plagioclase in the structural make-up of MT_{res} for the control (Table 2), a phase which is abundant (*ca* 25%) in $MT_{45\text{-}75}$. This demonstrated that the plagioclase phase, as anorthite $CaAl_2Si_2O_8$, underwent considerable, near complete dissolution during the acid leaching step in 0.63M HNO_3 at 95°C, and had therefore most likely contributed substantially to Ca, Al and Si co-extraction to solution. Other phases that may have also contributed to Ca, Al and Si co-extraction, although to a much lesser extent, were chlorite and calcite, which were also not identified in MT_{res} for the control, and possibly amphibole (as hornblende), which may be expected to be present in greater proportion if it had not partially dissolved (Table 2). On this basis, a normalised $CaO\text{-}Al_2O_3$ chemographic diagram was drawn (Figure 6), illustrating (i) the ideal chemical compositions of the three major Ca, Al-bearing minerals, along with (ii) the experimental chemical composition of untreated $MT_{45\text{-}75}$, against the experimental chemical compositions of (iii) filtrates generated during the control experiment, and (iv) filtrates following dissolution under controlled acid (0.63M HNO_3) condition of MT_{tct} produced using the four ammonium salts at 550 °C. The diagram showed similarities in chemical compositions between the filtrate generated by the control experiment and an ideal plagioclase (as anorthite) mineral phase (32% CaO – 68% Al_2O_3). This congruence in elemental composition confirmed that the plagioclase phase contained in $MT_{45\text{-}75}$ has substantially contributed to Ca and Al in the filtrates. The plagioclase phase, as anorthite $CaAl_2Si_2O_8$, underwent considerable, near complete dissolution during the acid leaching step in 0.63M HNO_3 at 95°C. This finding does not necessarily imply that plagioclase is not reactive with ammonium salts during the thermochemical processing step.

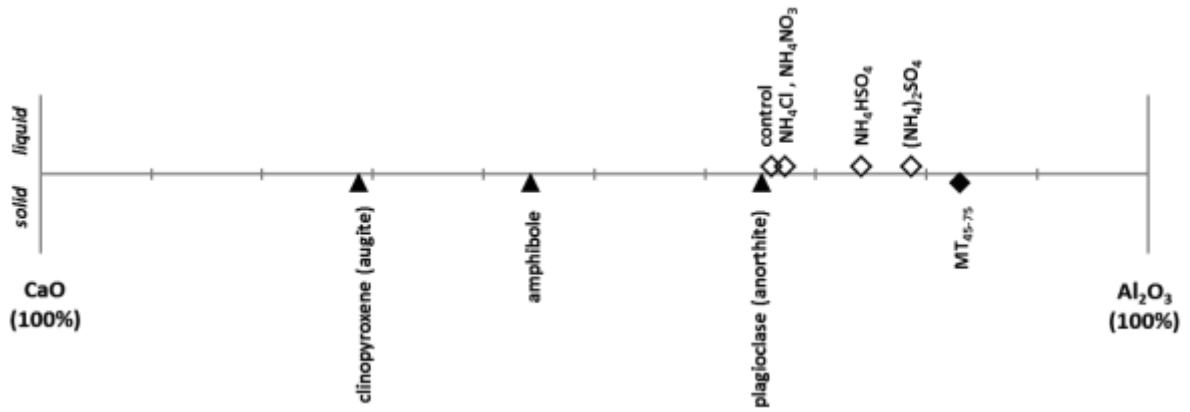

Figure 6. CaO-Al_2O_3 chemographic diagram illustrating (1) ideal chemical compositions of plagioclase (as anorthite), clinopyroxene (as augite), and amphibole minerals, (2) experimental chemical composition of untreated $MT_{45\text{-}75}$ (solid phases represented below the axis; closed triangle); and experimental chemical compositions of (3) filtrates generated during the control experiment and (4) filtrates following dissolution under controlled acid (0.63 M HNO_3) condition of MT_{tct} produced using the four ammonium salts (liquid phases represented above the axis; open diamond). Assumption has been made that only plagioclase (as anorthite), clinopyroxene (as augite), and amphibole minerals present in $MT_{45\text{-}75}$ can make a significant contribution to both Ca and Al extraction to solution after thermochemical treatment followed by dissolution.

3.3.2. Treatment experiments

TG was used to determine the thermal stability and phase transformations of $MT_{45\text{-}75}$, MT_{tct} and MT_{res}. Analysis of MT_{tct} was performed to assess the presence of unreacted reactant as well as confirm the formation of new mineral phases following thermochemical treatment. Analysis of MT_{res} following dissolution in HNO_3 was also conducted to confirm the efficiency of the dissolution procedure. The technique was combined with XRD and SEM to provide further insight on the physicochemical features of these materials.

TG analysis of untreated $MT_{45\text{-}75}$ was presented elsewhere [6]. In short, the TG curve was mostly constant with no distinctive events identified over the temperature range studied. This indicated that the mineral phases present in the sample had been thermally stable up to 1000 °C. A slight mass gain (<2%) was observed which was most likely due to the oxidation of Fe contained in the sample.

The TG curves obtained for thermal decomposition of the pure ammonium salts and the respective MT_{tct} and MT_{res} samples are compared in Figure 7. The curves of MT_{tct} produced using either NH_4NO_3 or NH_4Cl at 450-550 °C were mostly constant, with no distinctive events identified over the duration of the heating program (Figures 7A1 and 7B1). This indicated that the mineral phases present in the samples, including the newly-formed crystals, had been thermally stable up to 1000 °C. Another explanation for the stability of the TG curves of these MT_{tct} samples is that the new mineral phases may have been formed in such small quantities that their thermal characteristics could not be

identified. However, TG analysis of MT_{tct} produced with NH_4Cl at lower temperatures indicated the presence of unreacted reactant, with a significant mass loss (>35%) corresponding to the decomposition of NH_4Cl observed for the product produced at 350°C (Figure 7B1; curves a and b). The TG curves of the corresponding MT_{res} exhibited no mass loss (Figures 7A2 and 7B2). However, a slight mass gain (< 2%) was observed for MT_{tct} and MT_{res} produced at 550°C (Figure 7A1 to 7B2; curve e), which was most likely due to the oxidation of Fe, as discussed earlier for untreated tailings.

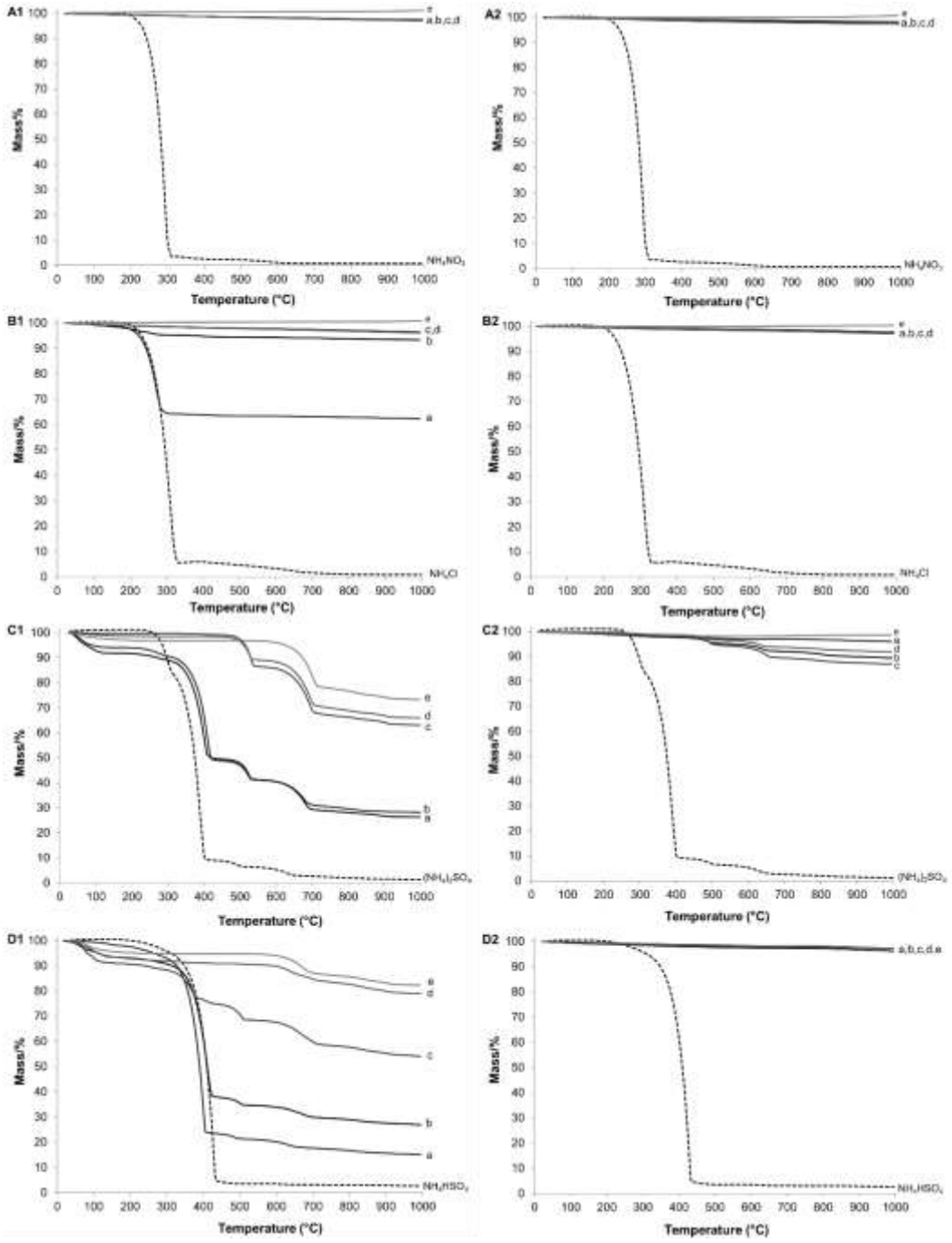

Figure 7. TG curves of MT_{tct} and MT_{res} generated via thermochemical treatment of $MT_{45\text{-}75}$ with NH_4NO_3 (A1-2), NH_4Cl (B1-2), $(NH_4)_2SO_4$ (C1-2) and NH_4HSO_4 (D1-2). Reaction temperature: a – 350 °C; b - 400 °C; c – 450 °C; d – 500 °C; e – 500 °C. (Figure C1 adapted and modified from [6]).

Clarification of the above discussion was given by FE-SEM, which provided evidence that new particles had formed during thermochemical treatment of MT_{45-75} with NH_4Cl (Figure 8) and NH_4NO_3 (Figure 9). MT_{tct} obtained using NH_4Cl consisted of anhedral particles (Figure 8A) which exhibited similar characteristics to those of MT_{45-75} described earlier (i.e. individual, irregularly-shaped particles with varying sizes and smooth surface topography [6]). However, upon treatment with NH_4Cl, the surfaces of particles were covered with epitaxial layers of sub-2µm poorly-formed crystals of varying habits (Figure 8B-D). The new crystals appeared to be growing out of the parent particles, which suggested that the surface of the primary particles may have been the site of nucleation. The growth pattern of the new crystals conformed to prism forms which were dichotomous in nature and comprised of hexagonal plate-like crystals with varying thicknesses, as well as twinned crystals with asymmetric features. These new crystals were also identified in the corresponding MT_{res} samples by FE-SEM (results not shown), which indicated that they had not, or only partially, dissolved under the dissolution conditions used. It is conceivable that metals present in the tailings that were extracted to solution (Figure 5) had reacted with NH_4Cl to form readily-soluble halide salt crystals (e.g. $CaCl_2$, $MgCl_2$, $AlCl_3$), whereas the newly-formed crystals seen by FE-SEM in both MT_{tct} and MT_{res} may have been water-insoluble Cl-bearing silicate and/or aluminosilicate minerals that had formed during thermochemical treatment.

In contrast, newly-formed particles that had developed during thermochemical treatment of MT_{45-75} with NH_4NO_3 were poorly crystallized, lacking sharp edges, and of sub-micron in size (Figure 9). In the same way as for the NH_4Cl experiments, the occurrence of some of these particles in the corresponding residual samples indicated that many of them had been poorly water-soluble. For the NH_4NO_3 experiments, it can also be speculated that metals present in the tailings that were extracted to solution (Figure 5) had reacted with NH_4NO_3 to form both readily-soluble metal nitrate salt crystals (e.g. $Ca(NO_3)_2$, $Mg(NO_3)_2$, $Al(NO_3)_3$, $5Ca(NO_3)_2 \bullet NH_4NO_3 \bullet 10H_2O$ double salts) as well as water-insoluble NO_3-bearing silicate and/or aluminosilicate minerals formed during thermochemical treatment.

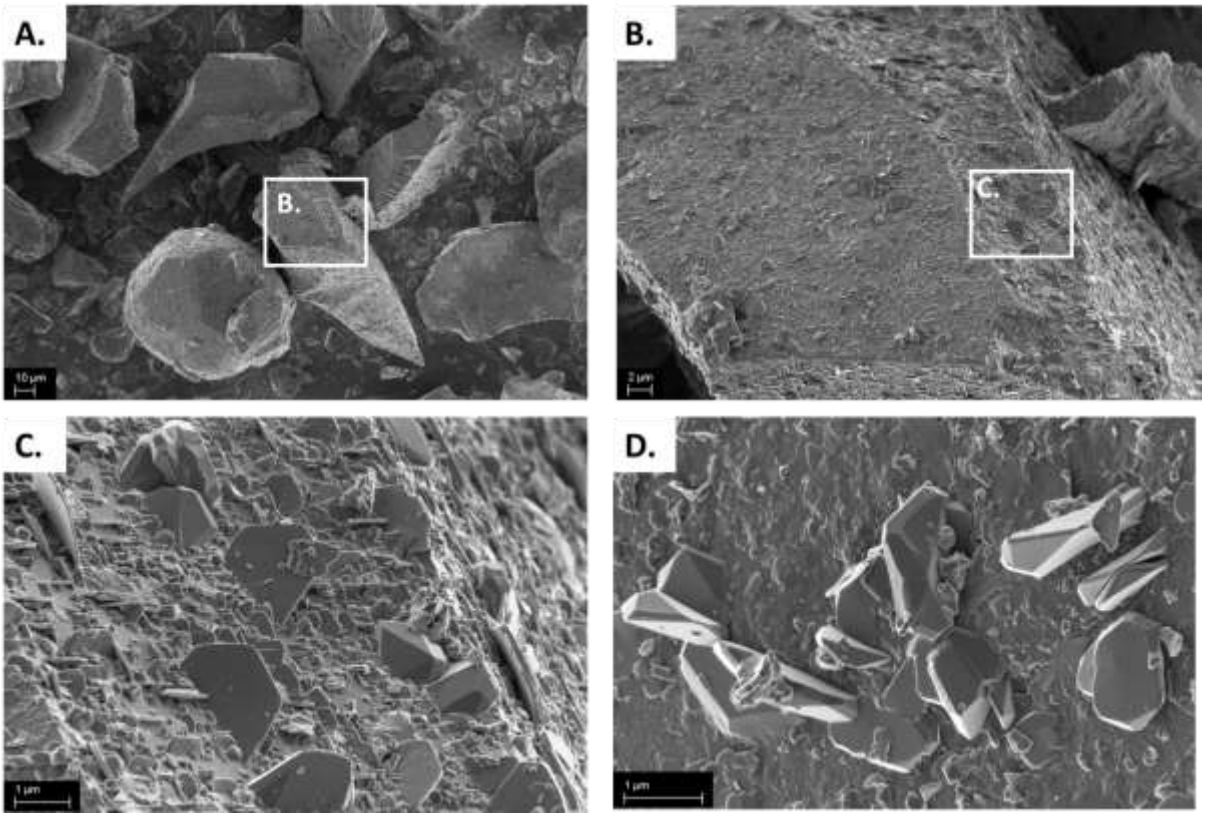

Figure 8. FE-SEM micrographs of MT_{tct} ($MT_{45\text{-}75}$:NH_4Cl of 2:6; 550 °C; 45 min) obtained at different magnifications (A. 1 000x; B. 6 000x; C. 28 000x; D. 40 000x).

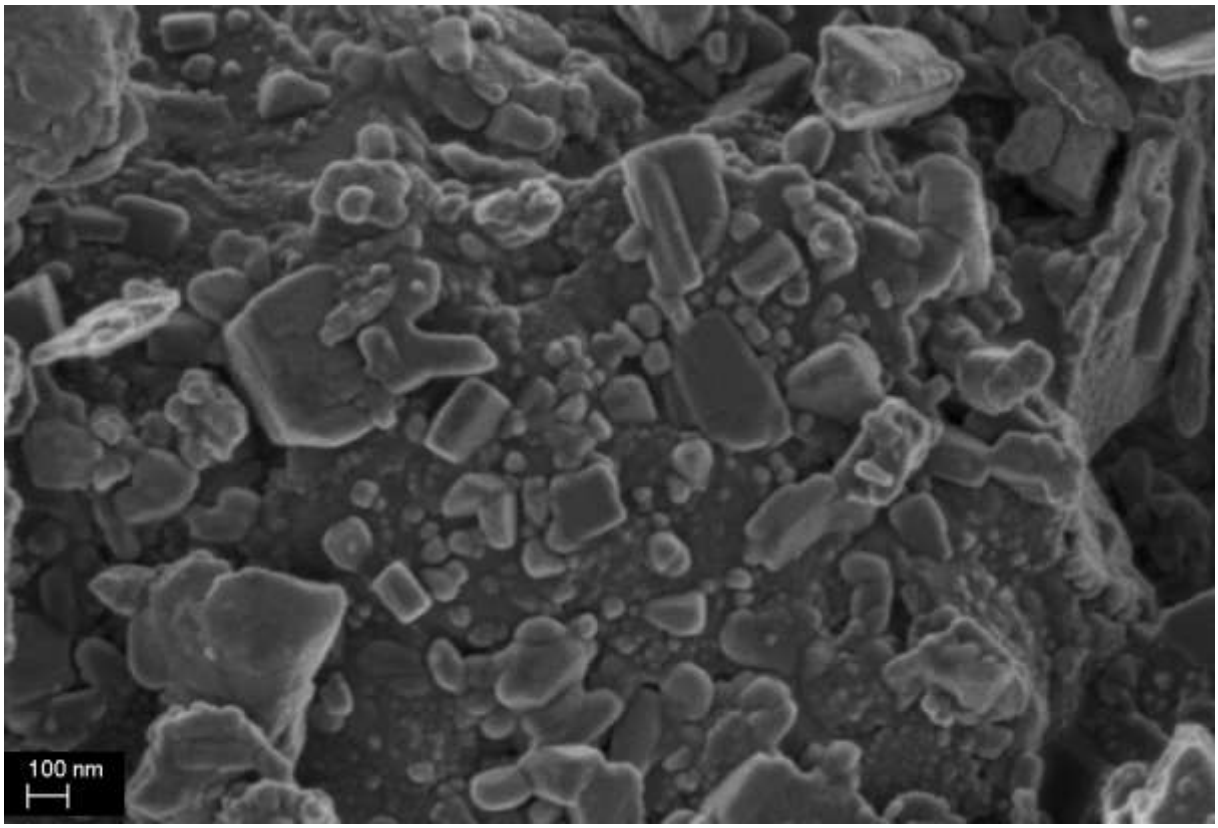

Figure 9. FE-SEM micrographs of newly-formed, poorly-crystallized particles present in MT_{tct} ($MT_{45\text{-}75}$:NH_4NO_3 of 2:6; 550 °C; 45 min; magnification: 100 000x).

The normalised CaO-Al_2O_3 chemographic diagram discussed earlier (Figure 6) also showed similarities in chemical compositions between the filtrates generated from the NH_4Cl and NH_4NO_3 experiments (33% CaO – 67% Al_2O_3) and the ideal plagioclase (as anorthite) mineral phase (32% CaO – 68% Al_2O_3). This congruence in elemental composition implied that the plagioclase phase contained in $MT_{45\text{-}75}$ was the main contributor to Ca and Al in the filtrates, owing to its dissolution during acid leaching. It also confirmed the limited solubility of the new crystals present in MT_{tct} for the thermochemical treatment with NH_4Cl and NH_4NO_3 identified by FE-SEM (Figures 8 and 9). Thermodynamic conditions that would favour the formation of readily-soluble halide (in the case of NH_4Cl) or metal nitrate (in the case of NH_4NO_3) salt crystals are therefore key to improve elemental extraction efficiencies, although this may not be chemically and/or economically feasible.

The TG curves of MT_{tct} generated from the reaction between $MT_{45\text{-}75}$ and the two sulphate salts ($(NH_4)_2SO_4$ and NH_4HSO_4; (Figure 7C1 and 7D1)) followed a similar trend; however, they were very different from those obtained when using the two other salts. The first mass loss observed at < 200 °C corresponds to the loss of water, and was found to be more evident for MT_{tct} produced from NH_4HSO_4 than MT_{tct} produced from $(NH_4)_2SO_4$. The loss of water from MT_{tct} formed from $(NH_4)_2SO_4$ was only observed in products formed at lower temperatures and was previously assigned to the presence of hygroscopic NH_4HSO_4 particles and/or metal sulphate hydrate species generated at ≤ 400°C [6].

The presence of NH_4HSO_4 in MT_{tct} formed using $(NH_4)_2SO_4$ at ≤ 400°C and NH_4HSO_4 at ≤ 450°C was indicated by the loss of NH_3 between 350 - 450 °C. These results implied incomplete decomposition of NH_4HSO_4 and $(NH_4)_2SO_4$ at these temperatures. Increasing the duration of thermochemical treatment did not appear to represent a viable option to improve decomposition and/or reactivity of these reactants, as indicated by the lower extraction efficiencies obtained for most elements (Figure 4) and the absence of better flowability of hardened MT_{tct} with longer thermochemical treatment.

Dissociation of ammonium metal sulphate phases into their respective metal sulphate phases is known to occur between 450 – 550 °C [36], and this phenomenon was observed in MT_{tct} formed using $(NH_4)_2SO_4$ at ≤ 500°C and NH_4HSO_4 at ≤ 450°C. The onset of decomposition of Fe, Cr and Al sulphates ($FeSO_4/Fe_2(SO_4)_3$, $Cr_2(SO_4)_3.xH_2O$, $Al_2(SO_4)_3$) occurs at temperatures ranging between 500-600 °C [36–38], while that of Mg sulphate ($MgSO_4$) takes place from 850 °C [39]. Although the TG curves of MT_{tct} obtained from the sulphate salts exhibited similarities, a smaller mass loss was observed for MT_{tct} using NH_4HSO_4 compared to $(NH_4)_2SO_4$, regardless of the reaction temperature. For example, 18 % mass loss was observed for MT_{tct} using NH_4HSO_4 (Figure 7D-e) *vs* 27 % mass loss for MT_{tct} using $(NH_4)_2SO_4$ (Figure 7C-e) at 550 °C. This suggested that the mass of metal sulphates

that formed during thermochemical treatment was greater when MT_{45-75} reacted with $(NH_4)_2SO_4$ than with NH_4HSO_4. This further confirmed that $(NH_4)_2SO_4$ was more reactive with mineral phases contained in MT_{45-75} than NH_4HSO_4. Furthermore, the TG curves confirmed our earlier conclusion drawn from the ICP data (Figure 5), that $(NH_4)_2SO_4$ is a more effective extracting agent than NH_4HSO_4.

As reported previously [6], in addition to irregularly-shaped, smooth particles of unreacted tailings, MT_{tct} produced using $(NH_4)_2SO_4$ contained numerous newly-formed, well-defined hexagonal structures that were either individual, or interlocked particles forming clusters of varying sizes. These hexagonal platy structures were characterized by grainy surfaces. They were most probably metal (Fe, Al, Cr, and/or Mg) sulphates, since metal sulphate crystals generally display hexagonal habits [40,41]. Similar hexagonal particles were also identified in MT_{tct} produced using NH_4HSO_4, except that they were generally smaller (Figure 10). The TG curves of the corresponding MT_{res} exhibited no mass loss (Figure 7D2), which indicated that the dissolution procedure was successful in achieving complete solubility of metal sulphate species formed during thermochemical treatment. In contrast, MT_{res} obtained from $(NH_4)_2SO_4$ showed presence of small amounts of undissolved ammonium-metal sulphate and/or metal sulphate species, which may be ascribed to differences in the solubility of formed metal sulphate species during thermochemical treatment (Figure 7C2).

The normalised CaO-Al_2O_3 chemographic diagram (Figure 6) also depicted a shift towards higher Al_2O_3 concentrations when thermochemical treatment made use of sulphate-based salts, with the shift being more pronounced for $(NH_4)_2SO_4$ than NH_4HSO_4. While the reactivity of plagioclase with these two salts could not be substantiated, the reactivity of at least one Al-bearing mineral present in MT_{45-75} was required to explain the observed shift along the axis. Possible sources may have included spinel group minerals and/or chlorite, although this could not be determined in this study.

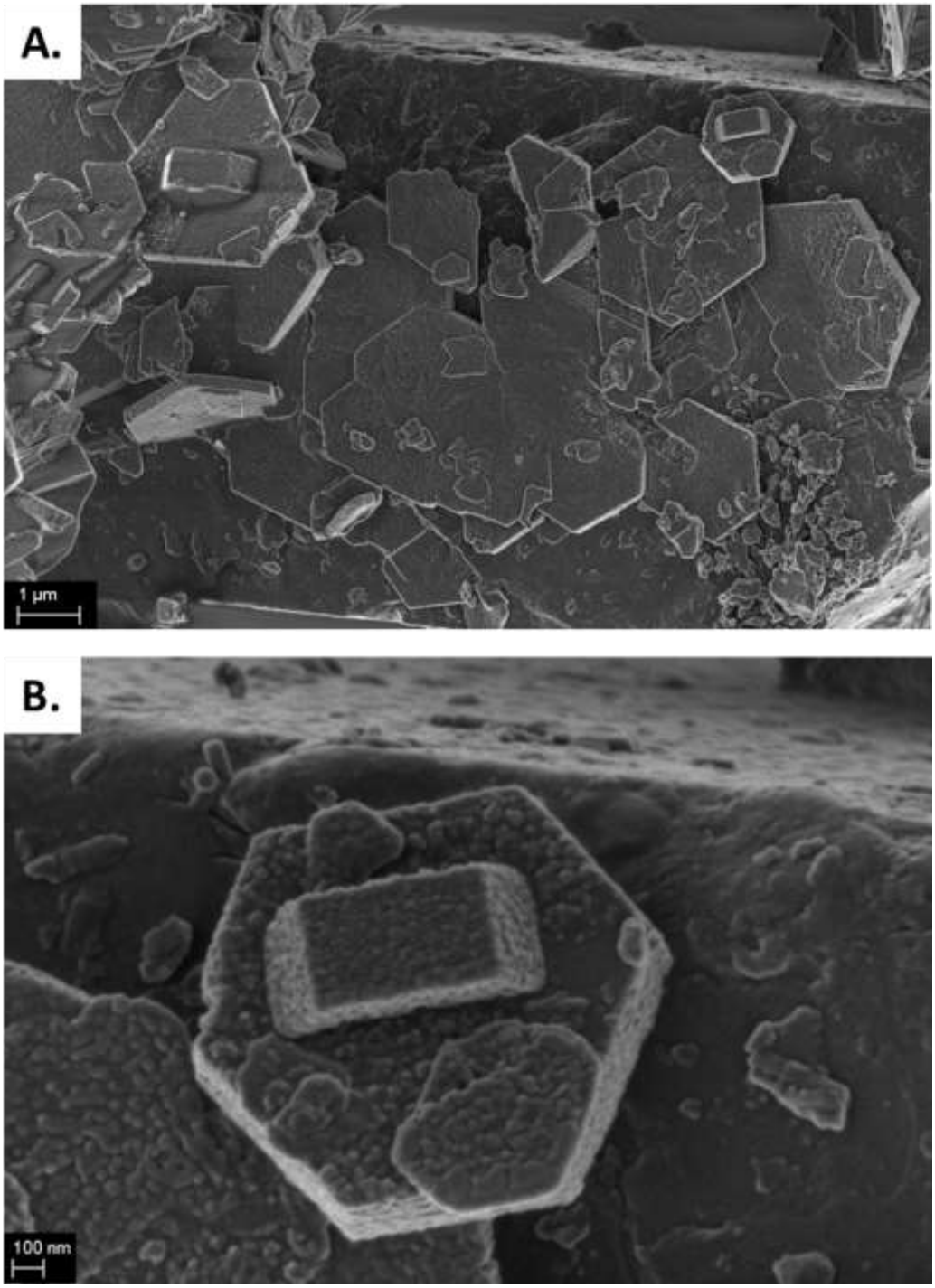

Figure 10. FE-SEM micrographs of MT_{tct} ($MT_{45\text{-}75}$:NH_4HSO_4 of 2:6; 550 °C; 45 min) obtained at different magnifications (A. 20 000x; B. 100 000x).

Table 2. Mineralogical composition of MT_{45-75} and of the non-dissolved residues (MT_{res}) obtained following (1) aqueous dissolution only (0.63M HNO_3 at 95 °C for 6h; Control), and (2) thermochemical treatment (MT_{45-75}:ammonium salt of 2:6; 45 min; 550 °C) followed by aqueous dissolution (0.63M HNO_3 at 95 °C for 6h).

Mineral group (mineral)	MT_{45-75} Untreated tailings	MT_{res}		
		Control	NH_4Cl	$(NH_4)_2SO_4$
Spinel group minerals[a]				
(magnetite + chromite+ulvöspinel)	29.5	33.9	52.7	49.3
Orthopyroxene, mostly enstatite	27.8	54.2	34.6	39.9
Feldspar (Plagioclase, as anorthite)	**25.2**	**1.2**	**1.0**	**1.3**
Amphibole (Hornblende)	7.9	6.6	6.8	6.6
Chlorite	3.1			
Calcite	2.4			
Clinopyroxene (Augite)	1.7	1.0		
Mica (Biotite)	1.6	tc[b]	1.3	0.8
Clay (Talc)	1	1.5	3.7	2.2

[a] Minerals of the spinel group are traditionally known as oxides with the generic formula AB_2O_4, where the symbols A and B represent divalent (e.g. Fe^{2+}, Mg^{2+}, Mn^{2+}, Ni^{2+} or Zn^{2+}) and trivalent ions (Fe^{3+}, Al^{3+}, Cr^{3+} or the pair $(Fe^{2+}Ti^{4+})^{6+}$ respectively. Only three species are relevant to the Bushveld Complex: magnetite ($Fe^{2+}O.Fe^{3+}{}_2O_3$), chromite ($(Mg,Fe)O.(Cr,Al,Fe)_2O_3$) and ulvöspinel ($Fe^{2+}O.(Fe^{2+}Ti^{4+})O_3$) [25].

[b] trace

Selection of extracting agents

An attractive aspect of the integrated process, which aims at achieving the full potential of utilisation of PGM tailings and currently under development, is the possibility of recycling the extracting agent. It is therefore important to point out that the four tested extracting agents have distinct recovery characteristics.

Extracting agent: $(NH_4)_2SO_4$

$(NH_4)_2SO_4$ is a widely available, low-cost chemical agent that can be easily regenerated by crystallisation. These qualities, combined with the superior extraction results reported here, make it the most attractive extracting agent for this process. However, it was reported that temperatures exceeding 400-420 °C during thermochemical treatment may lead to irreversible decomposition and loss of $(NH_4)_2SO_4$, which was recognized by the release of SO_x in the product vapours from the thermochemical reaction between $(NH_4)_2SO_4$ and serpentine [42]. These authors found that temperatures greater than 400 °C were necessary for good kinetics of Mg extraction from

serpentinite rocks. However, this irreversible decomposition phenomenon is unfavourable for industrial application [21]. While our study did not show that elevated temperature had promoted a substantial increase in major element extraction efficiencies from PGM tailings, it had a substantial effect on the flowability characteristic of the reaction products (MT_{tct}) after thermochemical treatment. In particular, the current study confirmed our previous finding [6] where at temperatures ≥ 450 °C, MT_{tct} were free-flowing powders that were easily recovered. In contrast, lower temperatures led to MT_{tct} with a molten, viscous-like appearance when hot (i.e. immediately upon removal from the furnace), but hardening and 'fusing' to the walls of the crucibles upon cooling. Hardened solids from the thermochemical treatment of serpentinite and metaperidotite with $(NH_4)_2SO_4$ were also previously reported [21,35]. Free-flowing, powdery reaction products are understandably much easier to recover before the dissolution step. In the future, it will therefore be important to optimize the thermochemical step at lower temperatures (≤ 420 °C), with the intent of improving the flowability characteristic of MT_{tct}, to favour the possible scaling-up of the process. Using wet rather than dry $(NH_4)_2SO_4$ during thermochemical treatment may provide a possible improvement since this was found to promote the formation of light and fluffy, porous, and easy-to-dissolve reaction products from serpentine and metaperidotite, which were easily recovered from crucibles [21].

Extracting agent: NH_4HSO_4

In addition to promoting lower extraction efficiencies from PGM tailings than $(NH_4)_2SO_4$, NH_4HSO_4 also requires a more challenging and energy-consuming recovery procedure than $(NH_4)_2SO_4$ [43]. The authors discussed that NH_4HSO_4 regeneration by thermal decomposition of $(NH_4)_2SO_4$ can suffer from the corrosive nature of NH_4HSO_4 and thus would not be economically viable, whereas its regeneration by H_2SO_4 addition saturates the process with sulphate and results in a negative exergy balance.

Extracting agent: NH_4Cl

NH_4Cl can also be easily regenerated by crystallisation [24], in a similar way to $(NH_4)_2SO_4$. However, NH_4Cl reacted with PGM tailings to form a range of new crystals which exhibited poor solubility characteristics. Complete recovery of metals extracted from the tailings to the new crystals, and that of the chloride locked in these same crystals, could therefore not be achieved. This is an additional disadvantage to the low extraction efficiencies achieved for most major elements.

Extracting agent: NH_4NO_3

Although pure NH_4NO_3 is generally considered as a relatively stable chemical at ambient temperature and pressure [44], factors such as external heat and contamination may impose an explosion hazard following decomposition mechanisms that are often not yet unambiguously understood [45]. While its use in small amounts (i.e. 2 g) during thermochemical treatment of PGM tailings can be performed safely in our laboratory, it is not recommended to scale up the process to industrial size as heating or any ignition source, as well as contaminants locked in mineral waste, may cause violent combustion and explosion. For this reason, the use of NH_4NO_3 in this application should be avoided.

Conclusions

Thermochemical treatment of PGM tailings using ammonium salt can successfully extract major metals from tailings via the formation of mostly water-soluble, metal-containing species. The four ammonium salts exhibit varying degrees of reactivity with the primary minerals contained in tailings. The type of ammonium salt used strongly affects elemental extraction efficiencies, whereas the greatest effect of temperature is on the flowability characteristic of the reaction products after thermochemical treatment. Based on extraction efficiency and recycling potential, $(NH_4)_2SO_4$ represents the most promising extracting agent, with the best extraction efficiencies achieved for Al (*ca.* 60%) and Ca (*ca.* 80%), alongside Cr (*ca.* 29%), Fe (*ca.* 35%), Mg (*ca.* 25%) and Si (*ca.* 32%). The plagioclase phase, as anorthite $CaAl_2Si_2O_8$, undergoes considerable, near complete dissolution during the acid leaching step in 0.63M HNO_3 at 95°C and is the main contributor to Ca and Al in solution. This finding does not imply that plagioclase is not reactive with ammonium salts during the thermochemical processing step. Although the thermochemical method is not element-selective, the process offers the significant advantage of using a universal, low-cost and recyclable extracting agent to recover major elements from PGM tailings in a readily-available soluble form, which could be subsequently converted to value-added products.

Acknowledgments

This work is based on research supported by the Council for Geoscience, the South African Department of Mineral Resources (DMR), the University of Pretoria, and the Geological Society of South Africa (GSSA) Ante the GSSA REI Fund. S.M. was supported by a Masters' Block Grant Free Standing Scholarship from the National Research Foundation of South Africa (NRF). Any opinion,

finding, conclusion or recommendation expressed in this material is that of the authors and the NRF does not accept any liability in this regard.

References

1. Golev A, Lebre E, Corder G. The contribution of mining to the emerging circular economy - AusIMM Bulletin. AusIMM Bull. 2016. https://www.ausimmbulletin.com/feature/the-contribution-of-mining-to-the-emerging-circular-economy. Accessed August 2016.

2. Schreck M, Wagner J. Incentivizing secondary raw material markets for sustainable waste management. Waste Manag. 2017;67:354–9.

3. ETP SMR High Level Group. Strategic Research and Innovation Agenda. European Technology Platform for Sustainable Mineral Resources (ETP SMR). 2013; pp. 40.

4. Department of Science and Technology.National Waste R&D and Innovation Roadmap for South Africa: Phase 2 Waste RDI Roadmap. Trends in waste management and priority waste streams for the Waste RDI Roadmap. Department of Science and Technology: Pretoria. 2014; pp.47.

5. Meyer NA, Vögeli JU, Becker M, Broadhurst JL, Reid DL, Franzidis JP. Mineral carbonation of PGM mine tailings for CO_2 storage in South Africa: A case study. Miner Eng. 2014;59:45–51.

6. Mohamed S, van der Merwe EM, Altermann W, Doucet FJ. Process development for elemental recovery from PGM tailings by thermochemical treatment: Preliminary major element extraction studies using ammonium sulphate as extracting agent. Waste Manag. 2016;50:334–45.

7. Mohamed S, van der Merwe EM, Altermann W, Doucet FJ. Addendum to “Process development for elemental recovery from PGM tailings by thermochemical treatment: Preliminary major element extraction studies using ammonium sulphate as extracting agent” [Waste Manage. 50 (2016) 334–345]. Waste Manag. 2017;66:222–4.

8. Liu Y, Naidu R. Hidden values in bauxite residue (red mud): Recovery of metals. Waste Manag. 2014;34:2662–73.

9. Ma D, Wang Z, Guo M, Zhang M, Liu J. Feasible conversion of solid waste bauxite tailings into highly crystalline 4A zeolite with valuable application. Waste Manag. 2014;34:2365–72.

10. Chmielewski AG, Wawszczak D, Brykała M. Possibility of uranium and rare metal recovery in the Polish copper mining industry. Hydrometallurgy. 2016;159:12–8.

11. Muthukannan V, Praveen K, Natesan B. Fabrication and characterization of magnetite/reduced

graphene oxide composite incurred from iron ore tailings for high performance application. Mater Chem Phys. 2015;162:400–7.

12. Ghacham A Ben, Cecchi E, Pasquier L-C, Blais J-F, Mercier G. CO_2 sequestration using waste concrete and anorthosite tailings by direct mineral carbonation in gas--solid--liquid and gas--solid routes. J Environ Manage. 2015;163:70–7.

13. Vogeli J, Reid DL, Becker M, Broadhurst J, Franzidis JP. Investigation of the potential for mineral carbonation of PGM tailings in South Africa. Miner Eng. 2011;24:1348–56.

14. Jubilee Platinum. 2015. http://www.jubileeplatinum.com/investors-and-media/announcements/2015/15-dec-2015.php. Accessed 12 Feb 2016.

15. Implats. Mineral resource and mineral reserve statement 2015. 2015. http://financialresults.co.za/2015/implats-minerals-report-2015/chromium.php. Accessed 12 Feb 2016.16. Creamer M. Northam initiates R100m tailings retreatment project. In: Mining Weekly. 2017. http://www.miningweekly.com/article/northam-initiates-r100m-tailings-retreatment-project-2017-08-28/rep_id:3650. Accessed 30 Aug 2017.

17. Doucet FJ. Scoping study on CO_2 mineralization technologies. Contract Report No CGS-2011-007, commissioned by the South African Centre for Carbon Capture and Storage. 2011; pp.88.

18. Doucet FJ, Mohamed S, Neyt N, Castleman BA, van der Merwe EM. Thermochemical processing of a South African ultrafine coal fly ash using ammonium sulphate as extracting agent for aluminium extraction. Hydrometallurgy. 2016;166:174–84.

19. van der Merwe EM, Gray CL, Castleman BA, Mohamed S, Kruger RA, Doucet FJ. Ammonium sulphate and/or ammonium bisulphate as extracting agents for the recovery of aluminium from ultrafine coal fly ash. Hydrometallurgy. 2017;171:185–90.

20. Barnardo D. Aluminium. In: The Mineral Resources of South Africa. Wilson MGC, Anhaeusser CR, editors. 6th ed. Council for Geoscience, Pretoria, South Africa;1998. p. 46-52.

21. Romão IS, Gando-Ferreira LM, da Silva MMVG, Zevenhoven R. CO_2 sequestration with serpentinite and metaperidotite from Northeast Portugal. Miner Eng. 2016;94:104–14.

22. D'yachenko AN, Kraidenko RI. Processing oxide-sulfide copper ores using ammonium chloride. Russ J Non-Ferrous Met. 2010;51:377–81.

23. Andreev AA, D'yachenko AN, Kraidenko RI. Processing of oxidized nickel ores with ammonium chloride. Theor Found Chem Eng. 2011;45:521.

24. Nadirov RK, Syzdykova LI, Zhussupova AK, Usserbaev MT. Recovery of value metals from copper smelter slag by ammonium chloride treatment. Int J Miner Process. 2013;124:145–9.

25. Eales HV. The Bushveld Complex, an introduction to the geology and setting of the Bushveld Complex. Council for Geoscience, Pretoria, South Africa; 2014;pp. 214.

26. Erdey L, Gal S, Liptay G. Thermoanalytical properties of analytical-grade reagents: ammonium salts. Talanta. 1964;11:913–40.

27. Kosova DA, Emelina AL, Bykov MA. Phase transitions of some sulfur-containing ammonium salts. Thermochim Acta. 2014;595:61–6.

28. Olszak-Humienik M. On the thermal stability of some ammonium salts. Thermochim Acta. 2001;378:107–12.

29. Chi R, Zhang X, Zhu G, Zhou ZA, Wu Y, Wang C, et al. Recovery of rare earth from bastnasite by ammonium chloride roasting with fluorine deactivation. Miner Eng. 2004;17:1037–43.

30. Chaturvedi S, Dave PN. Review on thermal decomposition of ammonium nitrate. J Energ Mater. 2013;31:1–26.

31. Gunawan R, Zhang D. Thermal stability and kinetics of decomposition of ammonium nitrate in the presence of pyrite. J Hazard Mater. 2009;165:751–8.

32. Izato Y, Miyake A. Thermal decomposition of molten ammonium nitrate (AN). J Therm Anal Calorim. 2015;122:595–600.

33. Romão IS, Gando-Ferreira LM, Zevenhoven R. Combined extraction of metals and production of $Mg(OH)_2$ for CO_2 sequestration from nickel mine ore and overburden. Miner Eng. 2013;53:167–70.

34. Romão I, Gando-Ferreira LM, Zevenhoven R. Separation and recovery of valuable metals extracted from serpentinite during the production of $Mg(OH)_2$ for CO_2 sequestration. Miner Eng. 2015;77:25–33.

35. Nduagu E, Björklöf T, Fagerlund J, Wärnå J, Geerlings H, Zevenhoven R. Production of magnesium hydroxide from magnesium silicate for the purpose of CO_2 mineralisation-Part 1: Application to Finnish serpentinite. Miner Eng. 2012;30:75–86.

36. Nagaishi T, Ishiyama S, Matsumoto M, Yoshinaga S. Reactions between ammonium sulphate and metal oxides (metal= Cr, Mn and Fe) and thermal decomposition of the products. J Therm

Anal. 1984;29:121–9.

37. Bayer G, Kahr G, Müller-Vonmoos M. Reactions of ammonium sulphates with kaolinite and other silicate and oxide minerals. Clay Miner. 1982;17:271–83.

38. Crouse KA, Badri M. Thermal studies on chromium (II) salts. Thermochim Acta. 1991;177:239–51.

39. Tagawa H. Thermal decomposition temperatures of metal sulfates. Thermochim Acta. 1984;80:23–33.

40. Jambor JL, Grew ES, Roberts AC. New mineral names. Am Mineral. 1996;81:1513–8.

41. Debbarma M, Das S, Saha M. Effect of reducing agents on the structure of zinc oxide under microwave irradiation. Adv Manuf. 2013;1:183–6.

42. Highfield J, Lim H, Fagerlund J, Zevenhoven R. Mechanochemical processing of serpentine with ammonium salts under ambient conditions for CO_2 mineralization. RSC Adv. 2012;2:6542–8.

43. Romão I, Slotte M, Gando-Ferreira LM, Zevenhoven R. CO_2 sequestration with magnesium silicates—Exergetic performance assessment. Chem Eng Res Des. 2014;92:3072–82.

44. Oxley JC, Smith JL, Rogers E, Yu M. Ammonium nitrate: thermal stability and explosivity modifiers. Thermochim Acta. 2002;384:23–45.

45. Cagnina S, Rotureau P, Adamo C. Study of incompatibility of ammonium nitrate and its mechanism of decomposition by theoretical approach. AIDIC. 2013;31:823–8.

46. Nduagu EI, Highfield J, Chen J, Zevenhoven R. Mechanisms of serpentine-ammonium sulfate reactions: Towards higher efficiencies in flux recovery and Mg extraction for CO_2 mineral sequestration. RSC Adv. 2014;4:64494–505.

47. Jariwala M, Crawford J, LeCaptain DJ. In situ Raman spectroscopic analysis of the regeneration of ammonium hydrogen sulfate from ammonium sulfate. Ind Eng Chem Res.; 2007;46:4900–5

48. Lee CT, Sohn HY. Recovery of synthetic rutile and iron oxide from ilmenite ore by sulfation with ammonium sulfate. Ind Eng Chem Res. 1989;28:1802–8.

49. Kiyoura R, Urano K. Mechanism, Kinetics, and Equilibrium of Thermal Decomposition of Ammonium Sulfate. Ind Eng Chem Process Des Dev. 1970;9:489–94.

Supplementary material

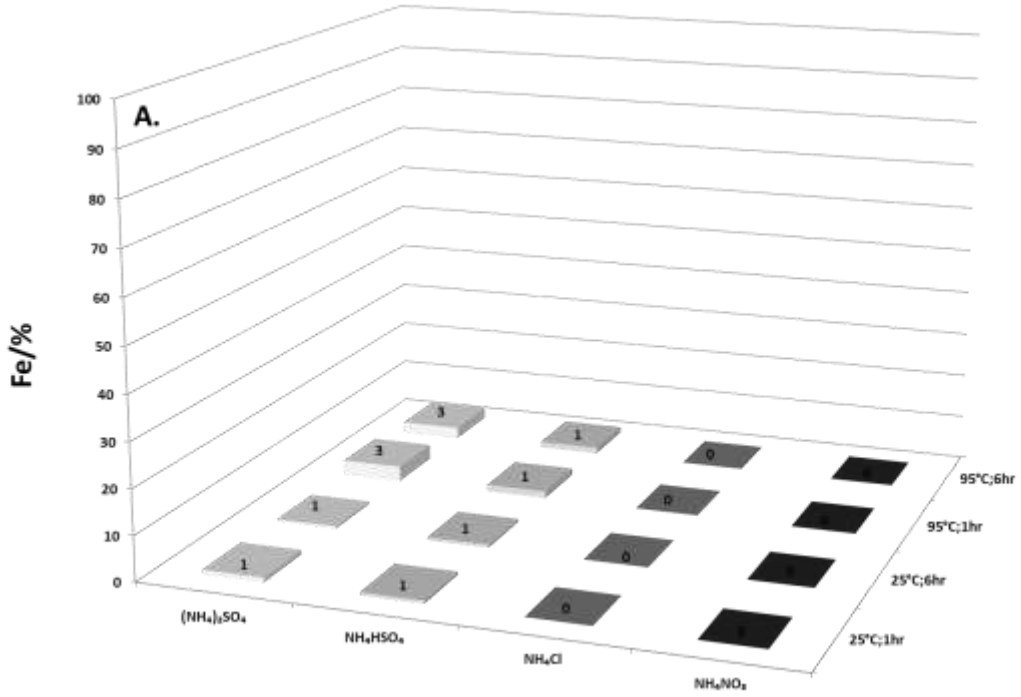

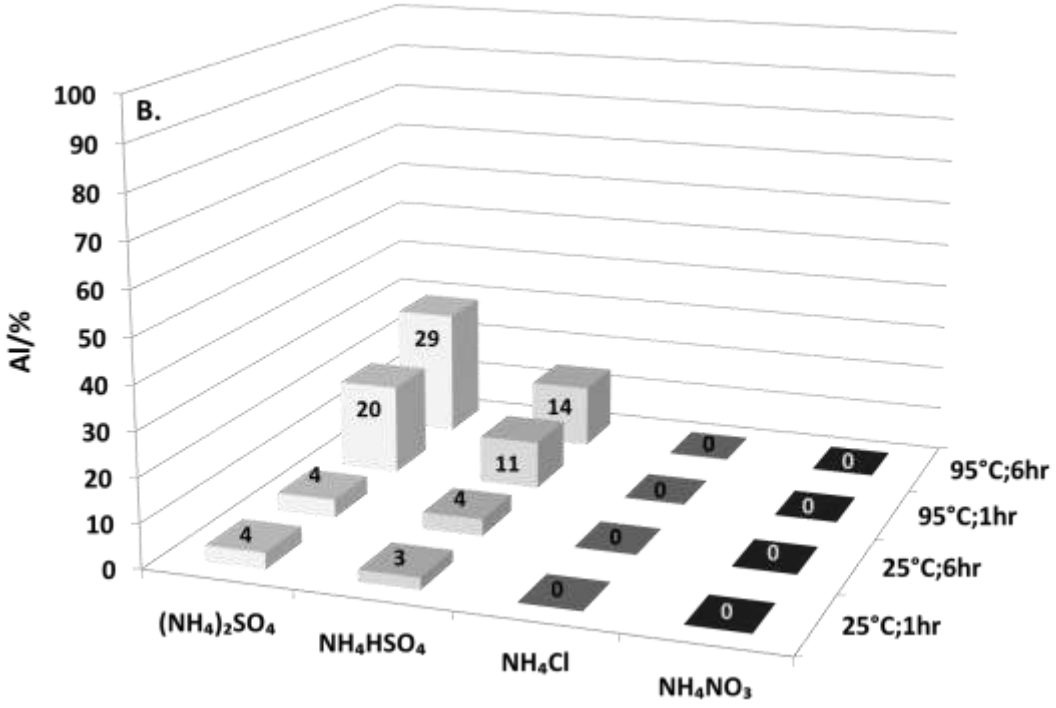

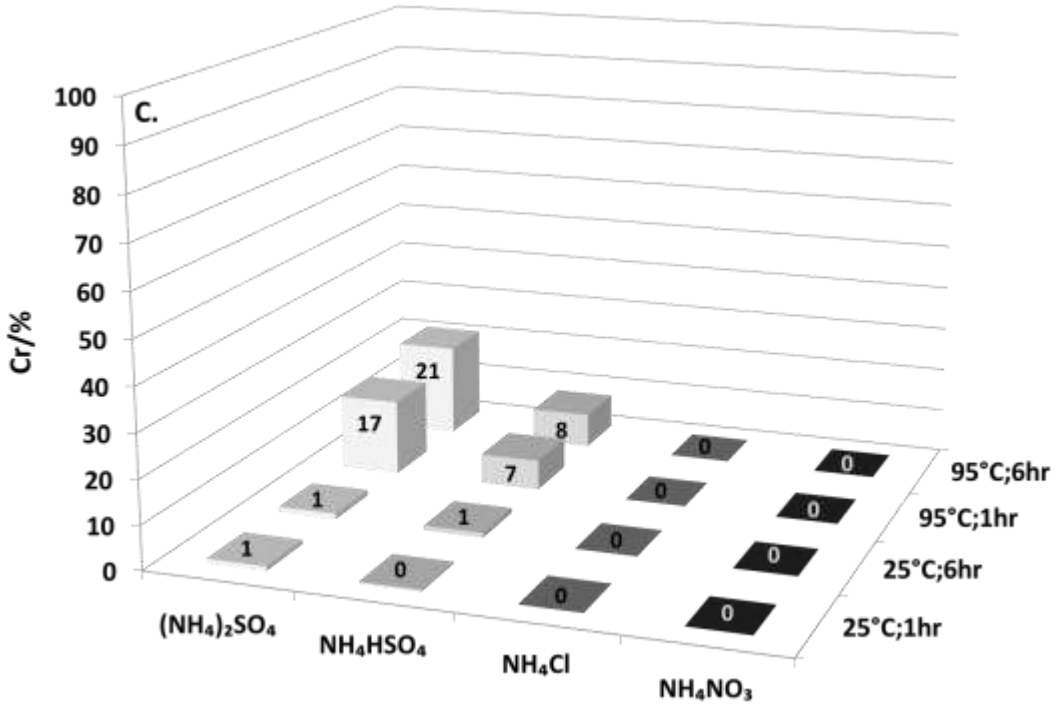
C.
Cr/%
100
90
80
70
60
50
40
30
20
10
0
21
17
8
7
1
1
1
0
0
0
0
0
0
0
0
95°C;6hr
95°C;1hr
25°C;6hr
25°C;1hr
(NH4)2SO4
NH4HSO4
NH4Cl
NH4NO3

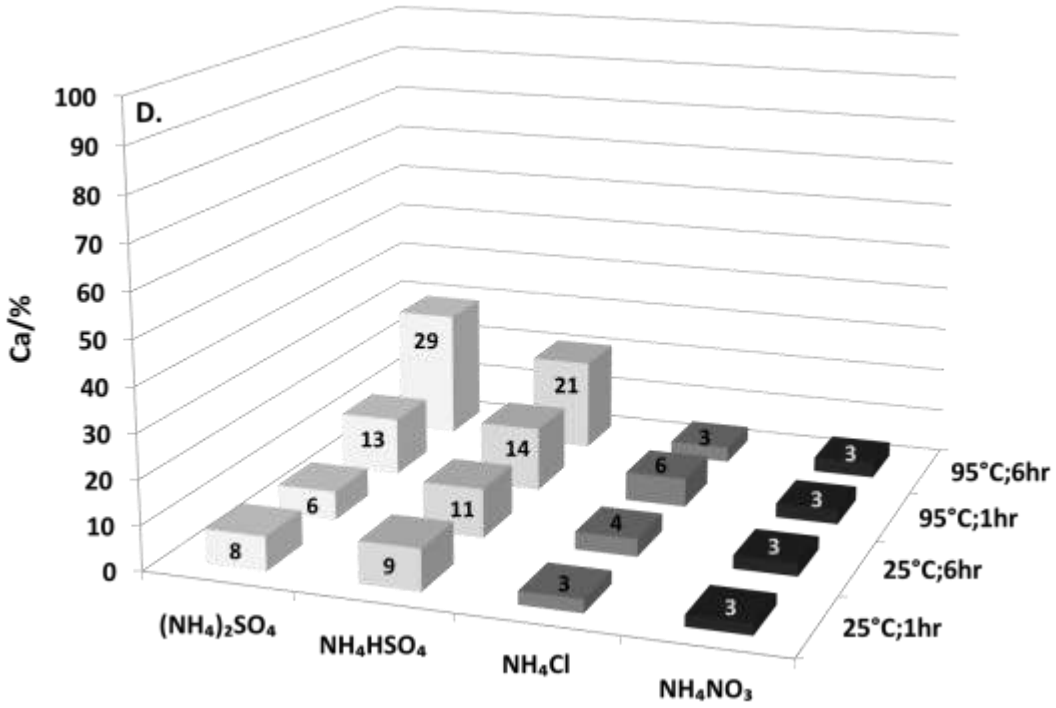
D.
Ca/%
100
90
80
70
60
50
40
30
20
10
0
29
21
13
14
6
11
8
9
3
6
4
3
3
3
3
3
95°C;6hr
95°C;1hr
25°C;6hr
25°C;1hr
(NH4)2SO4
NH4HSO4
NH4Cl
NH4NO3

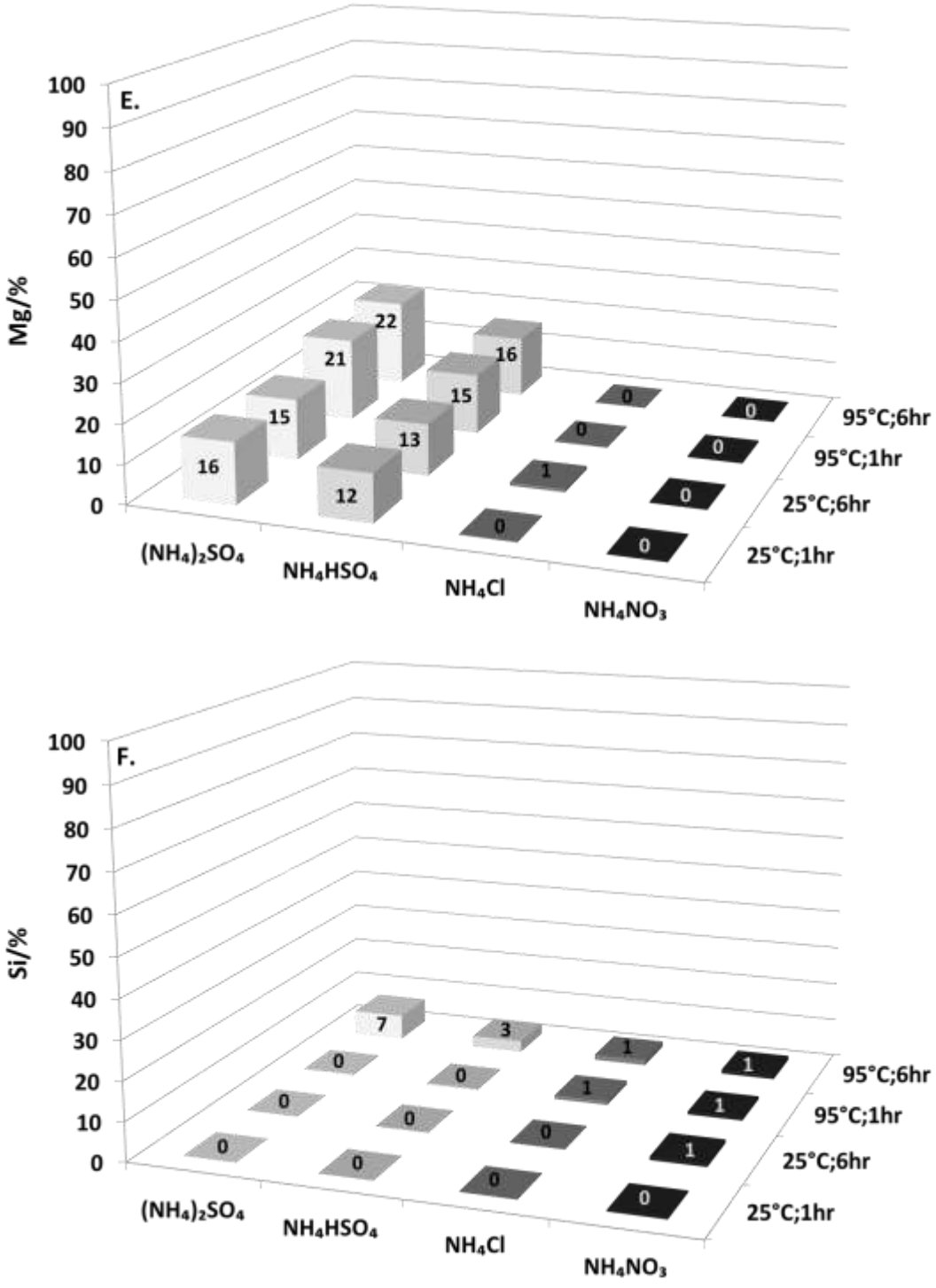

Supplementary Figure 1. Elemental extraction efficiencies when leaching MT_{tct} generated with all four salts at 550 °C (MT_{45-75}:salt of 2:6) in ultra-pure water at 25 °C and 95 °C, for 1h and 6h (3 g MT_{tct}/500ml; 850 rpm).